

PSEO: Optimizing Post-Hoc Stacking Ensemble Through Hyperparameter Tuning

Beicheng Xu¹, Wei Liu¹, Keyao Ding¹, Yupeng Lu¹, Bin Cui^{1*}

¹School of CS & Key Laboratory of High Confidence Software Technologies (MOE), Peking University, Beijing, China
{beichengxu, eularioal, maodeshi}@stu.pku.edu.cn, {xinkelyp, cui.bin}@pku.edu.cn

Abstract

The Combined Algorithm Selection and Hyperparameter Optimization (CASH) problem is fundamental in Automated Machine Learning (AutoML). Inspired by the success of ensemble learning, recent AutoML systems construct post-hoc ensembles for final predictions rather than relying on the best single model. However, while most CASH methods conduct extensive searches for the optimal single model, they typically employ fixed strategies during the ensemble phase that fail to adapt to specific task characteristics. To tackle this issue, we propose PSEO, a framework for post-hoc stacking ensemble optimization. First, we conduct base model selection through binary quadratic programming, with a trade-off between diversity and performance. Furthermore, we introduce two mechanisms to fully realize the potential of multi-layer stacking. Finally, PSEO builds a hyperparameter space and searches for the optimal post-hoc ensemble strategy within it. Empirical results on 80 public datasets show that PSEO achieves the best average test rank (2.96) among 16 methods, including post-hoc designs in recent AutoML systems and state-of-the-art ensemble learning methods.

Code — <https://github.com/PKU-DAIR/mindware>

Extended version — <https://arxiv.org/pdf/2508.05144v2>

1 Introduction

In recent years, machine learning has advanced in diverse application domains, such as computer vision (He et al. 2016; Jiang et al. 2024b), and recommendation systems (Wang et al. 2024; Chen et al. 2025). Despite these advancements, developing tailored solutions with strong performance remains a knowledge-intensive task, requiring careful selection of suitable ML algorithms and hyperparameter tuning. To lower barriers and streamline the deployment of machine learning applications, the AutoML community has introduced the Combined Algorithm Selection and Hyperparameter Optimization (CASH) problem (Thornton et al. 2013) and proposed several methods (Hutter, Kotthoff, and Vanschoren 2019; He, Zhao, and Chu 2021) to automate this optimization process. Furthermore, it’s widely acknowledged ensembling promising models often outperforms single ones (Feurer et al. 2015; Luo

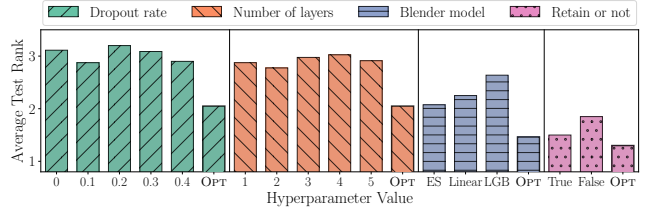


Figure 1: Average test rank of stacking across each hyperparameter’s values with other parameters fixed.

et al. 2024; Zhu et al. 2025). And ensemble strategies can be frequently found in the top solutions of prediction competitions (Koren 2009; Hoch 2015). As a result, recent AutoML systems (e.g., Auto-sklearn (Feurer et al. 2022), AutoGluon (Erickson et al. 2020), and VolcanoML (Li et al. 2023)) build post-hoc ensembles using base models from the optimization process of the optimal individual model and show better empirical results than the best single models.

Despite the effectiveness of those post-hoc ensemble designs, they typically employ a fixed ensemble strategy or leave it to the user to specify, rather than performing comprehensive optimization like with a single optimal model. However, as shown in Figure 1 and detailed in Appendix G, when we apply stacking ensembles, fixing other hyperparameters and performing a grid search for each hyperparameter separately, the tuned value according to validation performance (OPT) achieve higher average test ranks than other fixed-value strategies, demonstrating the potential of optimizing ensembles. Additionally, existing AutoML systems seldom explore base model selection for ensembles; instead, all available models or the best subset are simply used. Therefore, how to search for the optimal post-hoc ensemble solution, including base model selection and strategies for ensemble base models, remains an unresolved problem.

The optimization of post-hoc ensemble is non-trivial. When we attempt to characterize an ensemble strategy using hyperparameters and search for an optimal ensemble, two challenges arise: **C1**. Since the input for post-hoc ensembles is a discrete pool of pre-trained base models, selecting models for integration is a combinatorial optimization problem, where the hyperparameter space can be exceedingly large. As a result, it is challenging to reduce the number of hyper-

*Bin Cui is the corresponding author

parameters required to characterize the problem, enabling more efficient exploration. **C2**. It is challenging to fully realize the potential of the post-hoc ensemble and provide a flexible framework adaptable to various tasks, along with optional strategies for addressing specific issues.

In this paper, we propose PSEO, a new framework that optimizes post-hoc stacking ensemble through hyperparameter tuning. The contributions are summarized as follows: 1) To the best of our knowledge, PSEO is the first work to optimize post-hoc stacking ensemble through hyperparameter tuning. 2) To deal with **C1**, PSEO transforms the base model selection task into a binary quadratic programming problem and uses only two hyperparameters to control the optimization objective, achieving a trade-off between the diversity of selected base models and individual performance. 3) For **C2**, PSEO introduces the Dropout and Retain mechanisms to mitigate the problems of overfitting and feature degradation, respectively. 4) Instead of relying on fixed strategies, PSEO defines a hyperparameter space for post-hoc stacking ensembles and employs Bayesian optimization to search for the optimal strategy iteratively. Empirical results on 80 public datasets show that PSEO achieves the best average test rank (2.96) among 16 methods.

2 Background

2.1 Post-Hoc Ensemble

In post-hoc ensemble, we are given a fitted model pool $\mathbb{M} = \{m_1, m_2, \dots, m_n\}$, which consists of all base models that are trained on \mathcal{D}_{train} and validated during the search for the optimal individual model. The goal is to aggregate an optimal subset of models from \mathbb{M} with an ensembler $f(\cdot; \theta)$ to minimize a loss function \mathcal{L} in validation set \mathcal{D}_{val} , which is:

$$\min_{m_{i_1}, \dots, m_{i_n} \in \mathbb{M}; \theta} \mathcal{L}(f(m_{i_1}, m_{i_2}, \dots, m_{i_n}; \theta), \mathcal{D}_{val}) \quad (1)$$

Intuitively, a post-hoc ensemble needs to address two key problems: (1) how to select an appropriate subset of base models from the candidate pool \mathbb{M} , and (2) how to determine the best ensembler $f(\cdot; \theta)$ to produce the final output.

2.2 Stacking

Among different ensemble strategies (e.g., bagging (Dietterich 2000), boosting (Freund, Schapire et al. 1996), ensemble selection (Caruana et al. 2004)), we adopt stacking (Van der Laan, Polley, and Hubbard 2007) as the ensembler because: 1) It has shown excellent experimental results, outperforming other methods (Purucker and Beel 2023a). 2) Stacking offers inherent flexibility. 3) It’s a general framework, as commonly used methods can be considered special cases of one-layer stacking and serve as the blender model.

Recently, some AutoML systems like AutoGluon (Erickson et al. 2020), LightAutoML (Vakhrushev et al. 2022), and H2O (LeDell and Poirier 2020) adopt stacking for post-hoc ensemble, which trains a blender model to aggregate the predictions of a set of base models (Breiman 1996). Furthermore, in multi-layer stacking, predictions from each layer’s stacker models become inputs for the next layer, forming a hierarchical structure. Table 1 shows the stacking strategies

System	Base Model	Layers	Blender Model
AutoGluon	ALL	Multiple	Ensemble Selection
LightAutoML	BEST	One/Two	Weighted Avaraging
H2O	ALL/BEST	One	Linear/LightGBM/...

Table 1: Stacking strategy of current AutoML systems.

of the prominent open-source AutoML systems. We identify three common issues in their post-hoc stacking strategies.

Issue #1: Existing approaches lack an effective mechanism for selecting base models. Existing AutoML systems simply either include all models (ALL) or use the best-performing model from each algorithm class (BEST). However, both theory and experiments support that “many-could-be-better-than-all” in ensemble (Martinez-Munoz, Hernández-Lobato, and Suárez 2008; Zhou, Wu, and Tang 2002). On the other hand, it is generally accepted in the literature that diversity can help improve the performance of the ensemble (Bian and Chen 2021; Hansen and Salamon 1990; Ning et al. 2025), while selecting only the best subset lacks the assurance of base model diversity.

Issue #2: Existing works have not yet fully explored the potential of multi-layer stacking. There’s a curious trend that while multi-layer stacking is feasible, existing systems restrict themselves to two layers. For example, AutoGluon’s “best_quality” mode limits stacking to two layers. Similarly, LightAutoML reports using two-layer only for multi-class classification, which is the only case where consistent improvements are observed; one-layer stacking is used otherwise. H2O, meanwhile, only employs single-layer stacking. Moreover, there is also a risk of overfitting when aggregating base models, and existing systems lack effective solutions.

Issue #3: Existing approaches exhibit inflexible stacking strategies and lack optimization for specific tasks. Several parameters will determine the behavior and performance of stacking. For example, it involves the number of stacking layers and the choice of the blender model. However, only AutoGluon dynamically selects the number of stacking layers based on validation scores, while other systems fix it. As for the blender model of the final layer, AutoGluon and LightAutoML adopt fixed models, while H2O provides several choices for users to specify.

3 Method

In this section, we propose our method for post-hoc stacking ensemble optimization (PSEO). As shown in Figure 2, it first presents a **base model subset selection** algorithm with a trade-off between individual model performance and inter-model diversity. After that, PSEO builds a deep stacking ensemble with **Dropout** and **Retain** mechanisms to fully explore the potential of stacking. Finally, it defines a hyperparameter space for post-hoc ensemble, and uses a Bayesian optimizer to **search for the optimal ensemble** within it.

3.1 Base Model Subset Selection

In the scenario of post-hoc stacking, it is trivial to incorporate all available base models from the pool \mathbb{M} for stack-

ing. However, such a strategy lacks scalability. When provided with a large candidate model pool, stacking all models incurs significant overhead during both training and inference. In contrast, another approach selects only the best-performing models, which does not fully utilize the diversity of \mathbb{M} . Therefore, selecting the optimal base model subset for stacking is a meaningful problem worth investigating.

Nevertheless, the problem of selecting an optimal subset from a pool of candidate base models of size n is a variant of the constrained knapsack problem, which is NP-hard and impractical to solve exactly. To approximate a solution to this problem, we select a subset by focusing on two key factors: ensemble size and the trade-off between individual model performance and diversity among models.

We first use the pair-wise measures to represent the diversity of two given models. We utilize the definition in previous research (Poduval et al. 2024) that is supported by a theoretical framework and shows satisfactory empirical results. The diversity metric between two models (m_i, m_j) is:

$$D(m_i, m_j) = \mathbb{E}_{(x,y) \sim \mathcal{D}_{val}}(y - m_i(x)) \cdot (y - m_j(x)) \quad (2)$$

where for classification tasks, $m_i(x)$ is the predictive probability distribution and y is the one-hot label. For regression tasks, $m_i(x)$ is the predictive value and y is the label.

After that, we can build an error covariance matrix G , where $G_{ij} = D(m_i, m_j)$. The diagonal entries G_{ii} represent the mean square errors of model i on the validation data, while the off-diagonal entries G_{ij} quantify the error consistency between model i and j . Intuitively, a smaller diagonal entry indicates a better individual model, while a smaller off-diagonal entry suggests a larger error discrepancy between two models, implying greater diversity. Therefore, it's straightforward that a small value of $\sum_{ij} G_{ij}$ implies a good ensemble. Furthermore, to trade off between individual model performance and inter-model diversity, we introduce a weighting coefficient ω to G , where the weights of diversity and individual performance are ω and $1 - \omega$:

$$\tilde{G} = (1 - \omega) \cdot \text{diag}(G) + \omega \cdot (G - \text{diag}(G)) \quad (3)$$

Finally, given n candidate base models, selecting an optimal subset of size n' ($n' \leq n$) can now be formulated as:

$$\min_z z^T \tilde{G} z \quad \text{s.t.} \quad \sum z_i = n', \quad z_i \in \{0, 1\} \quad (4)$$

This binary quadratic programming (BQP) problem is NP-hard. To enable efficient approximation, we adopt a semidefinite programming (SDP) relaxation (Zhang et al. 2006). Specifically, we lift the binary variable into a positive semidefinite matrix $Z = zz^T$, and relax the rank-one and integrality constraints. The relaxed problem becomes:

$$\min_Z \text{Tr}(\tilde{G}Z) \quad \text{s.t.} \quad \text{Tr}(Z) = n', \quad Z \succeq 0, \quad Z \succeq zz^T \quad (5)$$

Equation 5 can be solved by standard semi-definite programming solvers. After that, we select the indices corresponding to the n' largest values in $\text{diag}(Z)$ and set their entries in z to 1, the rest to 0. When $z_i = 1$, the i -th model will be selected as one of the base models for ensemble.

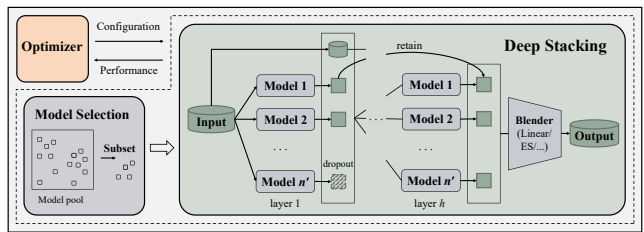


Figure 2: Overview of PSEO.

3.2 Deep Stacking Ensemble

After selecting the base model subset, we build a multi-layer stacking ensemble like the right part of Figure 2. Like AutoGluon, we reuse all base models as stacker models for each layer, which take inputs from the previous layer's predictive features and the original dataset. During training, we apply k -fold cross-validation to generate predictions for each stacker model, where each fold trains on part of the training set and predicts on the rest. This ensures stacker models always use out-of-fold (OOF) predictions and allow full training set utilization. During prediction, we average the outputs of k cross-validation models for each stacker to generate predictions on the validation or test set.

The above framework, referred to as deep stacking, can be viewed as a variant of a deep learning network, where each stacker model resembles a neuron. However, as the stacking depth increases, it becomes more complex, which can lead to two issues: **overfitting** and **feature degradation**. Overfitting refers to the phenomenon where stacking performs well on the training data but fails to generalize to test data. Feature degradation, on the other hand, describes the progressive decline in the quality of predictive features across layers. As a result, we introduce two mechanisms, Dropout and Retain, to mitigate the aforementioned issues, aiming to fully exploit the potential of deep stacking. The pseudo-code of the two mechanisms is provided in Appendix B.

Dropout. Consider a stacker model $S_{l,i}$ at layer l . If the predictive feature from the j -th stacker model $S_{l-1,j}$ of the previous layer is very close to the training set label, $S_{l-1,j}$ may become a dominating model in the training of $S_{l,i}$. It means there is a high probability that $S_{l,i}$ will overly rely on this predictive feature while neglecting other diverse features. For instance, a weighted model might assign a weight close to 1 to the j -th feature while setting others close to 0. Although it might effectively decrease the training loss, it may not generalize to test samples, leading to overfitting.

Therefore, motivated by the dropout in neural networks (Srivastava et al. 2014), we introduce the Dropout mechanisms in deep stacking. The key insight of Dropout is to encourage the ensemble to depend on diverse base models, preventing reliance on any dominating models that show strong training set performance. Specifically, receiving the predictive features from the previous layer, we first build a dropout mask for each predictive feature as:

$$m_i \sim \text{Bernoulli}\left(\frac{\mathcal{L}_{\min}}{\mathcal{L}_i} \gamma_0\right)$$

where γ_0 is the only parameter representing the dropout rate,

\mathcal{L}_{\min} represents the minimum loss with the training label among all predictive features from the previous layer, while \mathcal{L}_i denotes the loss of the i -th predictive feature. When m_i is 1, we exclude the i -th predictive feature and train the current stacker model using the retained features. Additionally, due to the randomness introduced by the dropout process, we perform multiple repetitions to ensure robustness. For each stacker model, we apply dropout independently to each fold of cross-validation. For the blender model, we repeatedly apply dropout and training, and compute an average of multiple blender models’ outputs for predicting. To sum up, by assigning higher dropout probabilities to features closer to the labels on the training set, we offer the opportunity to reduce the dominance of any single model in the ensemble.

Theorem 1. *Consider a set of uncorrelated base models predictions $\mathcal{Z} = \{z_1, z_2, \dots, z_{n'}\}$ in a weighted ensemble $z_{ens} = \sum_i \beta_i z_i$. The i -th prediction is dropout with rate d_i ($d_i = \rho_i \gamma_0$ and $\rho_1 = 1 \geq \rho_i \geq 0, i \in \{1, 2, \dots, n'\}$). If we perform N independent random samplings of \mathcal{Z} and get the average weight of each prediction, as $N \rightarrow \infty$, the proportion of z_1 ’s absolute average weight in the sum of all predictions’ (i.e. $|\tilde{\beta}_1| / \sum_{i=1}^{n'} |\tilde{\beta}_i|$) decreases as γ_0 increases.*

We give a proof of Theorem 1 in Appendix A, which shows that with sufficient sampling, averaging results from multiple training with Dropout can reduce the weight proportion of the predictive feature with the highest dropout probability in the weighted ensemble. In our scenario, the contribution of the feature with the lowest training loss will be reduced. Although the feature with the lowest training loss may not always be the dominating model, they are aligned with high probability. Even if not, as shown in Section 4.3, Dropout may still reduce the weight of the dominating model, as it tends to have lower training loss and thus a higher dropout probability compared to others.

Retain. When a stacker model $S_{l,i}$ generates low-quality predictive features on out-of-sample data—due to overfitting or poor training—and subsequent models fail to correct or compensate for these degraded features, errors can propagate across layers. This leads to a progressive decline in out-of-sample performance across layers, ultimately compromising the final output. We refer to this phenomenon as feature degradation in deep stacking.

To address this issue, we introduce the Retain mechanism. The insight of Retain to prevent the continued propagation of feature degradation after it occurs at a certain stacker model. Specifically, if Retain is enabled, it compares each stacker model’s predictive loss on the validation set with that of its counterpart from the previous layer (i.e., the stacker model at the same position and with the same configuration). If the current model underperforms, its output is replaced with that generated by its predecessor; otherwise, its output is retained. In this way, we offer the potential for the predictive features to progressively converge toward better representations across layers on data outside the training set.

3.3 Post-hoc Stacking Ensemble Optimization

Overall, post-hoc stacking can be divided into two stages: selecting a subset of base models and constructing a spe-

cific stacking ensemble based on the subset. Building upon the preceding design, we notice that several hyperparameters will determine the behavior of post-hoc stacking: 1) ensemble size and 2) diversity weight determine the size of the selected base model subset and the trade-off between individual performance and diversity within the subset. During the stacking stage, 3) the number of stacking layers and 4) the choice of blender model define the stacking structure; while 5) “retain or not” and 6) dropout rate control the training mechanisms to overcome the issues of overfitting and feature degradation. Therefore, we define the hyperparameter space of post-hoc stacking optimization as the combination of the above six hyperparameters. In order to identify the optimal post-hoc stacking strategy over the hyperparameter space, we employ the state-of-the-art black-box optimization technique, Bayesian Optimization (BO) (Snoek, Larochelle, and Adams 2012; Hutter, Hoos, and Leyton-Brown 2011). First, PSEO will collect the predictions of all models in the candidate pool on the validation set. At each iteration, it uses BO to suggest a new ensemble configuration. It then constructs a corresponding post-hoc ensemble on the training set and evaluates its performance on the validation set. After exhausting the budget, the best ensemble configuration found in the observations is returned. Appendix C shows the pseudo-code of PSEO and further details on the disk storage and reuse strategies to reduce computation.

3.4 Discussions

Extension. As a post-hoc ensemble framework, PSEO operates independently of the tuning algorithm used in the single best model searching stage, and can be applied to any AutoML system that produces a candidate model pool. PSEO also provides a general ensemble framework, within which other ensemble methods (e.g., ensemble selection) can be integrated as options of blender models.

Overhead Analysis. Suppose T_f is the average cost of fitting a stacker model on one fold, T_{p_1} and T_{p_2} are the average cost of a stacker model to predict on one fold of the training set and the validation set, respectively. During each iteration, the computation cost of training and validating a stacking is $kh n'(T_f + T_{p_1} + T_{p_2})$, where k is the fold number of cross-validation, h is the number of layers, and n' is the ensemble size. In practice, the training and validation of kn' stacker models in each layer can be executed in parallel, which can significantly reduce the computational cost.

Difference with Previous Methods. Methods such as Auto-WEKA (Thornton et al. 2013) and Autostacker (Chen et al. 2018) also conduct a searching of ensemble. We discuss the difference between PSEO and previous methods as follows: **D1.** The first difference lies in the search space. Auto-WEKA and Autostacker adopt an expanded search space covering both ensemble strategies and base model configurations. In contrast, PSEO adopts the post-hoc ensemble, where the search space covers base model selection and ensemble methods. **D2.** The main difference is in how the ensemble search space is explored. Auto-WEKA and Autostacker perform a joint search over both base models and their ensemble, leading to a combinatorial search space whose size grows exponentially with the maximum ensemble

Hyperparameter	Type	Range
Ensemble size	Int	[5, 50]
Diversity weight	Float	[0, 0.5]
Number of layers	Int	[1, 5]
Blender model	Categorical	{ES, Linear, LGB}
Dropout rate	Float	[0, 0.4]
Retain or not	Categorical	{True, False}

Table 2: Ensemble hyperparameter space of PSEO.

ble size. In contrast, PSEO represents base model subset selection using two key hyperparameters, allowing for only a linear increase in the number of candidate configurations.

4 Experiment

4.1 Experiment Setup

Baselines. We compare the proposed PSEO with 15 baselines. 1) The best model according to the validation metric (**Single-Best**); — *Three one-step ensemble learning methods*: 2) Ensemble optimization (EO) (Lévesque, Gagné, and Sabourin 2016) that maintains and updates an ensemble pool greedily; 3) **Autostacker** (Chen et al. 2018) that uses an evolutionary strategy to jointly search for the stacking structure and base model hyperparameters; 4) **Opt-DivBO** (Poduval et al. 2024) that maintains an ensemble selection and considers diversity while selecting the next model to train; — *Two post-hoc ensemble designs based on ensemble selection*: 5) Ensemble selection (ES) (Caruana et al. 2004); 6) **CMA-ES** (Purucker and Beel 2023b) that uses an evolutionary strategy to search for an optimal ensemble weight; — *Nine post-hoc ensemble designs based on stacking*: 7)-14) Based on the post-hoc stacking strategies adopted by existing AutoML systems, we consider three key hyperparameters. First, for base model selection, we adopt two commonly used strategies: (a) selecting all available models (ALL), and (b) selecting the best-performing model from each algorithm class (BEST). Second, we vary the number of stacking layers, considering both one-layer and two-layer configurations. Third, for the final blender model, we use two widely adopted approaches: ensemble selection (ES) and linear regression (Linear). By combining these choices, we obtain eight commonly used stacking strategies in existing AutoML systems (e.g., **ALL-Linear-L2** stacks all base models for two layers, and uses a linear blender for output); 15) We extracted AutoGluon’s “best_quality” ensemble strategy (**AutoGluon-**), which stacks all candidate models with up to two layers. The final number of layers is determined based on validation scores. If the time budget is limited, time is evenly allocated across layers, with models trained sequentially based on their validation scores.

Datasets and metrics. To compare PSEO with baselines, we use 80 real-world ML datasets from the OpenML repository (Vanschoren et al. 2014), 50 for classification tasks (CLS) and 30 for regression tasks (REG). The number of samples for CLS ranges from 1k to 110k, and that for REG ranges from 0.6k to 166k. Further dataset details can be

found in Appendix D. We report the test error for all classification tasks to measure misclassification rates, which equals $1 - accuracy$. While for regression tasks, we use *mean squared error* (MSE) to assess prediction error.

Construction of the base model pool. For all post-hoc ensemble methods, we construct the candidate base model pool \mathbb{M} using the AutoML system VolcanoML (Li et al. 2023). It defines a CASH search space encompassing algorithmic choices and feature engineering hyperparameters, which contains 100 hyperparameters in total (see Appendix E for details). We run the Bayesian optimization method of VolcanoML over this space and collect all evaluated models to form \mathbb{M} . In each iteration, models are fitted on the training set and evaluated on the validation set. All the fitted models are saved to disk for ensemble utilization.

Implementation Details. Each dataset undergoes a split into three distinct sets: training (60%), validation (20%), and test (20%). Table 2 shows the specific hyperparameter space of PSEO. The value ranges of the parameters can be adjusted based on the available budget or user preferences. We used 5-fold cross-validation for stacking training and performed dropout training of the blender model with the same number of repetitions. More implementation details for other baselines and the training process are provided in Appendix F.

For all post-hoc ensemble approaches, 3600 seconds are dedicated to constructing the candidate base model pool \mathbb{M} , yielding an average of 437 base models per task. For the baseline using a fixed post-hoc ensemble strategy, we execute it to completion. For methods that perform additional optimization during the post-hoc ensemble phase (CMA-ES, AutoGluon-, and PSEO), we allocate an extra 3600 seconds for ensemble-level optimization. For the three ensemble learning methods, we impose a total budget of 7200 seconds, due to the adoption of a one-step optimization strategy rather than a two-step post-hoc ensemble.

4.2 Effectiveness of Base Model Subset Selection

We first conduct an experiment to validate the effectiveness of PSEO’s base model subset selection algorithm. To investigate the impact of different ensemble size n' and diversity weight ω on the performance of stacking, we conduct a grid search over their feasible ranges. Specifically, n' is varied from 10 to 50 in increments of 10, while ω is varied from 0 to 0.5 with a step size of 0.1. For each combination of n' and ω , we generate a corresponding subset of base models and apply a one-layer stacking with Linear as the blender model. Then, the optimal combination (OPT) is selected based on validation performance and evaluated on the test set. We compare its test errors with those of 30 fixed hyperparameter combinations. Furthermore, we include comparisons with strategies commonly employed in AutoML systems, namely: ALL and BEST. Figure 3 presents the average test ranks of stacking ensembles constructed using base models selected by the different strategies. Each region represents a method, with color intensity and the number indicating the average rank (lighter is better). The 5×6 grid in the bottom-left corresponds to a grid search over n' and ω . The surrounding L-shaped region marks the optimal combinations selected on the validation set (OPT). The two blocks

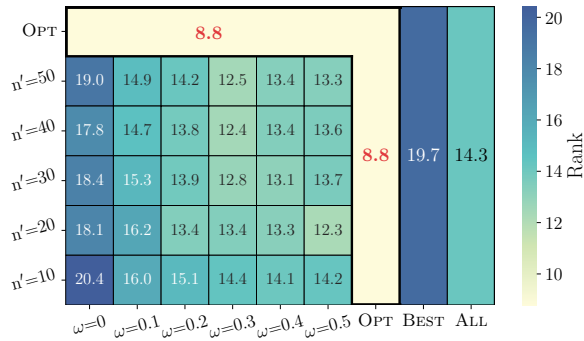


Figure 3: Average test ranks of stacking with different base model subset selection methods across 80 datasets.

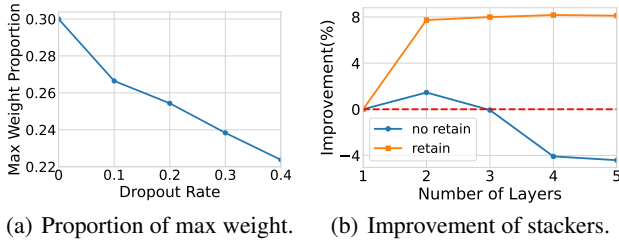


Figure 4: Effectiveness of Dropout and Retain mechanisms.

on the far right represent the BEST and ALL strategies.

We derive three observations from the results: 1) Ensembles based on low-diversity models show inferior performance. For instance, all the $\omega = 0$ strategies and BEST yield average ranks between 17.8 and 20.4. 2) PSEO’s base model selection mostly outperforms ALL and BEST, with 18 and 29 wins out of 30 configurations, respectively. 3) Tuning n' and ω leads to significant improvements, with OPT achieving a rank of 8.8 vs. 12.3 for the second-best baseline. The superiority of OPT stems from two factors: 1) it balances individual model performance and inter-model diversity with diversity weights, as further demonstrated in Appendix H. 2) it optimizes the ensemble size and diversity weight to achieve a task-specific base model selection strategy.

4.3 Effectiveness of Dropout and Retain

This section evaluates the impact of Dropout and Retain mechanisms. Here, we select 30 base models with a diversity weight of 0.3 and use ES as the blender model.

In Figure 4(a), for each dropout rate γ_0 ranging from 0 to 0.4, we trained the ES five times, averaged the weights, and reported the average proportion of the largest base model weight across 80 tasks. We can observe that as γ_0 increases, the largest weight shows a decreasing trend. Appendix I further shows that as the dropout rate increases, the gap between the training and test errors gradually narrows, indicating a reduction in overfitting. In Figure 4(b), we compute the average test error of stacker models’ predictive features at each layer, and report each layer’s average improvement rate relative to the first layer across 80 tasks. It is observed that without the Retain mechanism, feature quality peaks at the

second layer and subsequently deteriorates. In contrast, with the Retain mechanism, the predictive features show a more significant improvement, and no obvious degradation is observed as the number of layers increases. Appendix J provides further analysis of how predictive feature quality affects ensemble performance, concluding that in higher-level stacking, Retain significantly benefits the ensemble.

4.4 Comparison with Baselines

This section compares PSEO with state-of-the-art baselines on 80 real-world CASH problems. Table 3 shows the average test rank across different datasets, from which we can get five observations: 1) Ensemble indeed helps improve the performance of CASH results. The average rank of Single-Best is only 10.79, the lowest among all methods. 2) Among the ensemble learning methods, direct search for an ensemble (Autostacker, EO) is ineffective. This is because the huge search space, covering both ensemble and model hyperparameters, is challenging to optimize with Autostacker’s evolutionary algorithm or EO’s greedy update strategy. OptDivBO achieves a rank of 7.56, outperforming Autostacker (9.69) and EO (10.36), as it introduces ensemble selection to update the ensemble pool, thereby avoiding EO’s instability caused by including poor models during optimization. 3) Among all post-hoc ensemble methods, stacking shows great potential. AutoGluon-, ALL-ES-L2, and ALL-Linear-L1 achieve ranks between 6.19 and 6.36, higher than ES (7.78) and CMA-ES (8.53). This is because ES relies on a fixed greedy strategy, which inherently limits its upper bound, and CMA-ES may lead to overfitting. 4) We observe that stacking all models (ALL-**-*) outperforms stacking the best ones (BEST-**-*), as it fully leverages the diversity in \mathcal{M} . However, stacking all models incurs substantial costs, with single-layer stacking taking over an hour on average and multi-layer stacking becoming even more unacceptable. 5) Among all methods, PSEO significantly outperforms the others. While the second-best baseline achieves a rank of 6.19, the rank of PSEO is 2.96. The specific loss per dataset per method is shown in Appendix N.

We attribute the superiority of PSEO to three key factors: 1) As demonstrated in Section 4.2, it provides a customized base model selection for different tasks. 2) Dropout and Retain mechanisms mitigate the issues of overfitting and feature degradation, enhancing the potential of deep stacking ensembles. We conduct ablation studies of them in Appendix L. 3) Through optimization, PSEO builds task-specific stacking structures. As shown in Appendix G, optimizing stacking hyperparameters yields significant benefits.

Normalised Improvement. To further investigate our results, we use boxplots of the normalized improvement to visualize the distribution of relative performance for all methods across 80 datasets in Figure 5. Specifically, for each dataset, 1 corresponds to the minimum test loss achieved among all methods on it, and 0 corresponds to the test loss of Single-Best. If Single-Best is the best, we penalize the relative performance of worse methods to -10. We can conclude that PSEO has better relative performance distributions than all the baselines (see the medians and whiskers).

	Single-Best	EO	Autostacker	OptDivBO	ES	CMA-ES	ALL-ES-L1	ALL-ES-L2	ALL-Linear-L1
CLS	9.44	9.12	9.46	7.10	7.36	8.14	7.44	5.86	<u>5.72</u>
REG	13.03	12.43	10.07	8.33	8.47	9.17	8.07	6.90	7.43
ALL	10.79	10.36	9.69	7.56	7.78	8.53	7.67	6.25	6.36

	ALL-Linear-L2	BEST-ES-L1	BEST-ES-L2	BEST-Linear-L1	BEST-Linear-L2	AutoGluon-	PSEO
CLS	7.36	7.50	7.28	8.26	6.74	6.18	2.56
REG	7.23	9.73	7.80	9.40	7.43	<u>6.20</u>	3.63
ALL	7.31	8.34	7.47	8.69	7.00	<u>6.19</u>	2.96

Table 3: Average test rank across 50 classification tasks (CLS), 30 regression tasks (REG), and all tasks (ALL) for 16 methods. A smaller rank is better. The best methods are shown in bold, while the second-best methods are underlined.

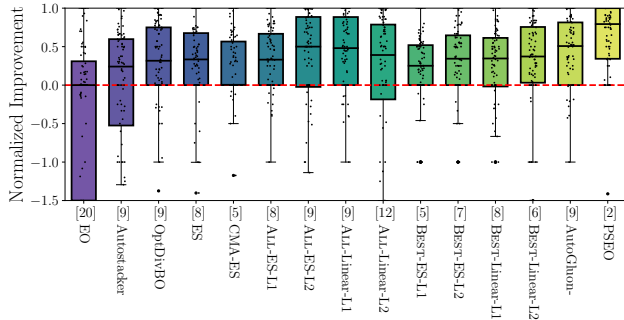


Figure 5: Normalised Improvement Boxplots: Higher is better. Each dot represents a dataset. The number in square brackets counts the outliers that are not shown in the plot.

	Single-Best	AutoGluon	PSEO
CLS	2.36	1.82	1.38
REG	2.63	2.03	1.33
ALL	2.46	1.90	1.36

Table 4: Average test rank in AutoGluon’s search space.

4.5 Comparison with AutoGluon

AutoGluon represents a state-of-the-art AutoML system with multi-layer stacking. The “best_quality” mode is not only AutoGluon’s best-performing mode but also surpasses all other AutoML systems in predictive accuracy (Gijssbers et al. 2024). To align with its ensemble strategy, AutoGluon employs a more compact CASH search space compared to VolcanoML. Therefore, for a fairer comparison, we replicated its search space, which includes 108 zero-shot models with priorities. We use AutoGluon to train base models for up to 1 hour, then allocate the remaining time within the 2-hour limit to optimize the ensemble with PSEO. AutoGluon is given a 2-hour budget using “best_quality”. The average test rank in 80 datasets is shown in Table 4, where we also include Single-Best as a baseline. We can conclude that both AutoGluon and PSEO outperform Single-Best, and PSEO is the best, with an average rank of 1.36. Additionally, we calculate the improvements in test loss achieved by PSEO and AutoGluon over Single-Best across all datasets, which

are 10.4% and 4.0% on average, respectively. To evaluate the statistical significance of PSEO, we conduct a Wilcoxon signed-rank test for the improvements of the two methods, where the value $p = 0.002 \leq 0.05$, indicating that PSEO is statistically significantly better than AutoGluon. To sum up, the consistent success of PSEO across candidate pools derived from two systems (VolcanoML and AutoGluon) highlights its robustness and general applicability.

5 Related Work

One-step Ensemble learning. Some methods directly search for an ensemble of models in a single step. AutoWEKA (Thornton et al. 2013) adopts a search space covering both ensemble and model hyperparameters, and solves it with Bayesian optimization. Ensemble Optimization (Lévesque, Gagné, and Sabourin 2016) maintains a fixed-size ensemble pool and optimizes each model in turn. Autostacker (Chen et al. 2018) and Neural ensemble search (Zaidi et al. 2021) focus on generating a complex ensemble via evolutionary search. Another type of work (Shen et al. 2022; Poduval et al. 2024) maintains and updates an ensemble selection with consideration of model diversity.

Ensemble Selection. Many AutoML systems, like AutoSklearn (Feurer et al. 2015), Auto-Pytorch (Zimmer, Lindauer, and Hutter 2021), and MLJAR (Płońska and Płoński 2021) utilize ensemble selection (Okun 2009). It iteratively adds models from the pool with replacement to maximize the ensemble performance. CMA-ES (Purucker and Beel 2023b) and Q(D)O-ES (Purucker et al. 2023) improve upon ES through choosing models with evolutionary algorithms.

6 Conclusion

In this paper, we propose PSEO, an efficient optimization framework to tune the post-hoc stacking ensemble. In PSEO, we proposed three components: a base model subset selection algorithm with a trade-off between individual model performance and inter-model diversity, a deep stacking ensemble with Dropout and Retain mechanisms to fully explore the potential of multi-layer stacking, and finally a Bayesian optimizer to search for the optimal ensemble strategy. We evaluated PSEO on 80 public datasets and demonstrated its superiority over competitive baselines.

7 Acknowledgement

This work is supported by National Natural Science Foundation of China (U23B2048, U22B2037).

References

- Bian, Y.; and Chen, H. 2021. When does diversity help generalization in classification ensembles? *IEEE Transactions on Cybernetics*, 52(9): 9059–9075.
- Breiman, L. 1996. Stacked regressions. *Machine learning*, 24: 49–64.
- Caruana, R.; Niculescu-Mizil, A.; Crew, G.; and Ksikes, A. 2004. Ensemble selection from libraries of models. In *Proceedings of the twenty-first international conference on Machine learning*, 18.
- Chen, B.; Wu, H.; Mo, W.; Chattopadhyay, I.; and Lipson, H. 2018. Autostacker: A compositional evolutionary learning system. In *Proceedings of the genetic and evolutionary computation conference*, 402–409.
- Chen, L.; Gao, C.; Lei, J.; Du, X.; Shi, X.; Luo, H.; Jin, D.; Li, Y.; and Wang, M. 2025. Privacy-preserving recommendation with coarse-grained spatiotemporal contexts. *Science China Information Sciences*, 68(4): 140104.
- Dietterich, T. G. 2000. Ensemble methods in machine learning. In *International workshop on multiple classifier systems*, 1–15. Springer.
- Erickson, N.; Mueller, J.; Shirkov, A.; Zhang, H.; Larroy, P.; Li, M.; and Smola, A. 2020. AutoGluon-Tabular: Robust and Accurate AutoML for Structured Data. arXiv:2003.06505.
- Feurer, M.; Eggenberger, K.; Falkner, S.; Lindauer, M.; and Hutter, F. 2022. Auto-sklearn 2.0: Hands-free automl via meta-learning. *Journal of Machine Learning Research*, 23(261): 1–61.
- Feurer, M.; Klein, A.; Eggenberger, K.; Springenberg, J.; Blum, M.; and Hutter, F. 2015. Efficient and robust automated machine learning. *Advances in neural information processing systems*, 28.
- Freund, Y.; Schapire, R. E.; et al. 1996. Experiments with a new boosting algorithm. In *icml*, volume 96, 148–156. Citeseer.
- Gijsbers, P.; Bueno, M. L.; Coors, S.; LeDell, E.; Poirier, S.; Thomas, J.; Bischl, B.; and Vanschoren, J. 2024. Amlb: an automl benchmark. *Journal of Machine Learning Research*, 25(101): 1–65.
- Hansen, L. K.; and Salamon, P. 1990. Neural network ensembles. *IEEE transactions on pattern analysis and machine intelligence*, 12(10): 993–1001.
- He, K.; Zhang, X.; Ren, S.; and Sun, J. 2016. Deep residual learning for image recognition. In *Proceedings of the IEEE conference on computer vision and pattern recognition*, 770–778.
- He, X.; Zhao, K.; and Chu, X. 2021. AutoML: A survey of the state-of-the-art. *Knowledge-based systems*, 212: 106622.
- Hoch, T. 2015. An Ensemble Learning Approach for the Kaggle Taxi Travel Time Prediction Challenge. In *DC@PKDD/ECML*.
- Hutter, F.; Hoos, H. H.; and Leyton-Brown, K. 2011. Sequential model-based optimization for general algorithm configuration. In *International Conference on Learning and Intelligent Optimization*, 507–523. Springer.
- Hutter, F.; Kotthoff, L.; and Vanschoren, J. 2019. *Automated machine learning: methods, systems, challenges*. Springer Nature.
- Jiang, H.; Shen, Y.; Li, Y.; Xu, B.; Du, S.; Zhang, W.; Zhang, C.; and Cui, B. 2024a. Openbox: A Python toolkit for generalized black-box optimization. *Journal of Machine Learning Research*, 25(120): 1–11.
- Jiang, R.; Zheng, G.-C.; Li, T.; Yang, T.-R.; Wang, J.-D.; and Li, X. 2024b. A Survey of Multimodal Controllable Diffusion Models. *Journal of Computer Science and Technology*, 39(3): 509–541.
- Koren, Y. 2009. The bellkor solution to the netflix grand prize. *Netflix prize documentation*, 81(2009): 1–10.
- LeDell, E.; and Poirier, S. 2020. H2o automl: Scalable automatic machine learning. In *Proceedings of the AutoML Workshop at ICML*, volume 2020, 24.
- Lévesque, J.-C.; Gagné, C.; and Sabourin, R. 2016. Bayesian hyperparameter optimization for ensemble learning. In *Proceedings of the Thirty-Second Conference on Uncertainty in Artificial Intelligence*, 437–446.
- Li, Y.; Shen, Y.; Zhang, W.; Chen, Y.; Jiang, H.; Liu, M.; Jiang, J.; Gao, J.; Wu, W.; Yang, Z.; et al. 2021. Openbox: A generalized black-box optimization service. In *Proceedings of the 27th ACM SIGKDD conference on knowledge discovery & data mining*, 3209–3219.
- Li, Y.; Shen, Y.; Zhang, W.; Zhang, C.; and Cui, B. 2023. VolcanoML: speeding up end-to-end AutoML via scalable search space decomposition. *The VLDB Journal*, 32(2): 389–413.
- Luo, F.-M.; Xu, T.; Lai, H.; Chen, X.-H.; Zhang, W.; and Yu, Y. 2024. A survey on model-based reinforcement learning. *Science China Information Sciences*, 67(2): 121101.
- Martinez-Munoz, G.; Hernández-Lobato, D.; and Suárez, A. 2008. An analysis of ensemble pruning techniques based on ordered aggregation. *IEEE Transactions on Pattern Analysis and Machine Intelligence*, 31(2): 245–259.
- Ning, Q.; Guo, C.; Liu, K.; Tang, J.; Zhang, S.; Zeng, W.; and Zhao, X. 2025. Dual Sequence Modeling for Knowledge Tracing. *Data Science and Engineering*, 1–12.
- Okun, O. 2009. *Applications of supervised and unsupervised ensemble methods*, volume 245. Springer Science & Business Media.
- Płońska, A.; and Płoński, P. 2021. MLJAR: State-of-the-art automated machine learning framework for tabular data. *Version 0.10*, 3.
- Poduval, P.; Patnala, S. K.; Oberoi, G.; Srivasatava, N.; and Asthana, S. 2024. Cash via optimal diversity for ensemble learning. In *Proceedings of the 30th ACM SIGKDD Conference on Knowledge Discovery and Data Mining*, 2411–2419.

Purucker, L.; and Beel, J. 2023a. Assembled-OpenML: Creating Efficient Benchmarks for Ensembles in AutoML with OpenML. arXiv:2307.00285.

Purucker, L. O.; and Beel, J. 2023b. CMA-ES for post hoc ensembling in AutoML: a great success and salvageable failure. In *International Conference on Automated Machine Learning*, 1–1. PMLR.

Purucker, L. O.; Schneider, L.; Anastacio, M.; Beel, J.; Bischl, B.; and Hoos, H. 2023. Q (D) O-ES: Population-based quality (diversity) optimisation for post hoc ensemble selection in AutoML. In *International Conference on Automated Machine Learning*, 10–1. PMLR.

Shen, Y.; Lu, Y.; Li, Y.; Tu, Y.; Zhang, W.; and Cui, B. 2022. Divbo: diversity-aware cash for ensemble learning. *Advances in Neural Information Processing Systems*, 35: 2958–2971.

Snoek, J.; Larochelle, H.; and Adams, R. P. 2012. Practical bayesian optimization of machine learning algorithms. In *Advances in neural information processing systems*, 2951–2959.

Srivastava, N.; Hinton, G.; Krizhevsky, A.; Sutskever, I.; and Salakhutdinov, R. 2014. Dropout: a simple way to prevent neural networks from overfitting. *The journal of machine learning research*, 15(1): 1929–1958.

Thornton, C.; Hutter, F.; Hoos, H. H.; and Leyton-Brown, K. 2013. Auto-WEKA: Combined selection and hyperparameter optimization of classification algorithms. In *Proceedings of the 19th ACM SIGKDD international conference on Knowledge discovery and data mining*, 847–855.

Vakhrushev, A.; Ryzhkov, A.; Savchenko, M.; Simakov, D.; Damdinov, R.; and Tuzhilin, A. 2022. LightAutoML: AutoML Solution for a Large Financial Services Ecosystem. arXiv:2109.01528.

Van der Laan, M. J.; Polley, E. C.; and Hubbard, A. E. 2007. Super learner. *Statistical applications in genetics and molecular biology*, 6(1).

Vanschoren, J.; Van Rijn, J. N.; Bischl, B.; and Torgo, L. 2014. OpenML: networked science in machine learning. *ACM SIGKDD Explorations Newsletter*, 15(2): 49–60.

Wang, G.; Li, X.; Guo, Z.-Y.; Yin, D.-W.; and Ma, S. 2024. SMEC: Scene Mining for E-Commerce. *Journal of Computer Science and Technology*, 39(1): 192–210.

Zaidi, S.; Zela, A.; Elsken, T.; Holmes, C. C.; Hutter, F.; and Teh, Y. 2021. Neural ensemble search for uncertainty estimation and dataset shift. *Advances in Neural Information Processing Systems*, 34: 7898–7911.

Zhang, Y.; Burer, S.; Nick Street, W.; Bennett, K. P.; and Parrado-Hernández, E. 2006. Ensemble Pruning Via Semi-definite Programming. *Journal of machine learning research*, 7(7).

Zhou, Z.-H.; Wu, J.; and Tang, W. 2002. Ensembling neural networks: many could be better than all. *Artificial intelligence*, 137(1-2): 239–263.

Zhu, J.; Zhao, X.; Sun, Y.; Song, S.; and Yuan, X. 2025. Relational data cleaning meets artificial intelligence: A survey. *Data Science & Engineering*, 10(2).

Zimmer, L.; Lindauer, M.; and Hutter, F. 2021. Autopytorch: Multi-fidelity metalearning for efficient and robust autodl. *IEEE transactions on pattern analysis and machine intelligence*, 43(9): 3079–3090.

Reproducibility Checklist

1. General Paper Structure

- 1.1. Includes a conceptual outline and/or pseudocode description of AI methods introduced (yes/partial/no/NA) **yes**
- 1.2. Clearly delineates statements that are opinions, hypothesis, and speculation from objective facts and results (yes/no) **yes**
- 1.3. Provides well-marked pedagogical references for less-familiar readers to gain background necessary to replicate the paper (yes/no) **yes**

2. Theoretical Contributions

- 2.1. Does this paper make theoretical contributions? (yes/no) **yes**

If yes, please address the following points:

- 2.2. All assumptions and restrictions are stated clearly and formally (yes/partial/no) **yes**
- 2.3. All novel claims are stated formally (e.g., in theorem statements) (yes/partial/no) **yes**
- 2.4. Proofs of all novel claims are included (yes/partial/no) **yes**
- 2.5. Proof sketches or intuitions are given for complex and/or novel results (yes/partial/no) **yes**
- 2.6. Appropriate citations to theoretical tools used are given (yes/partial/no) **yes**
- 2.7. All theoretical claims are demonstrated empirically to hold (yes/partial/no/NA) **yes**
- 2.8. All experimental code used to eliminate or disprove claims is included (yes/no/NA) **yes**

3. Dataset Usage

- 3.1. Does this paper rely on one or more datasets? (yes/no) **yes**

If yes, please address the following points:

- 3.2. A motivation is given for why the experiments are conducted on the selected datasets (yes/partial/no/NA) **yes**
- 3.3. All novel datasets introduced in this paper are included in a data appendix (yes/partial/no/NA) **NA**

- 3.4. All novel datasets introduced in this paper will be made publicly available upon publication of the paper with a license that allows free usage for research purposes (yes/partial/no/NA) **NA**
- 3.5. All datasets drawn from the existing literature (potentially including authors' own previously published work) are accompanied by appropriate citations (yes/no/NA) **yes**
- 3.6. All datasets drawn from the existing literature (potentially including authors' own previously published work) are publicly available (yes/partial/no/NA) **yes**
- 3.7. All datasets that are not publicly available are described in detail, with explanation why publicly available alternatives are not scientifically satisfying (yes/partial/no/NA) **NA**
- 4.9. This paper formally describes evaluation metrics used and explains the motivation for choosing these metrics (yes/partial/no) **yes**
- 4.10. This paper states the number of algorithm runs used to compute each reported result (yes/no) **yes**
- 4.11. Analysis of experiments goes beyond single-dimensional summaries of performance (e.g., average; median) to include measures of variation, confidence, or other distributional information (yes/no) **yes**
- 4.12. The significance of any improvement or decrease in performance is judged using appropriate statistical tests (e.g., Wilcoxon signed-rank) (yes/partial/no) **yes**
- 4.13. This paper lists all final (hyper-)parameters used for each model/algorithm in the paper's experiments (yes/partial/no/NA) **yes**

4. Computational Experiments

- 4.1. Does this paper include computational experiments? (yes/no) **yes**

If yes, please address the following points:

- 4.2. This paper states the number and range of values tried per (hyper-) parameter during development of the paper, along with the criterion used for selecting the final parameter setting (yes/partial/no/NA) **yes**
- 4.3. Any code required for pre-processing data is included in the appendix (yes/partial/no) **yes**
- 4.4. All source code required for conducting and analyzing the experiments is included in a code appendix (yes/partial/no) **yes**
- 4.5. All source code required for conducting and analyzing the experiments will be made publicly available upon publication of the paper with a license that allows free usage for research purposes (yes/partial/no) **yes**
- 4.6. All source code implementing new methods have comments detailing the implementation, with references to the paper where each step comes from (yes/partial/no) **yes**
- 4.7. If an algorithm depends on randomness, then the method used for setting seeds is described in a way sufficient to allow replication of results (yes/partial/no/NA) **NA**
- 4.8. This paper specifies the computing infrastructure used for running experiments (hardware and software), including GPU/CPU models; amount of memory; operating system; names and versions of relevant software libraries and frameworks (yes/partial/no) **yes**

Appendix

A Theoretical Proofs

In this section, we provide the proof of Theorem 1.

Proof sketches: To prove Theorem 1, we 1) first establish Lemma 1, showing that the expected value of the sampled weight is the product of the probability of retention and the original weight without Dropout, leveraging the orthogonality of predictions and linearity of expectation. 2) Next, for Theorem 2, we apply the law of large numbers to demonstrate that the average estimator converges almost surely to the product as the times of sampling $\rightarrow \infty$, using the result from the lemma. 3) Finally, with Lemma 1 and Theorem 2, we can represent the proportion of $|\hat{\beta}_1|$ in the sum of all others, and prove it's monotonically non-decreasing with respect to γ_0 .

Lemma 1. Consider a set of uncorrelated base models predictions $\mathcal{Z} = \{z_1, z_2, \dots, z_{n'}\}$ in an ensemble with prediction $z_{ens} = \sum_i \beta_i z_i$. If all the z_i are orthogonal, we perform random samplings of \mathcal{Z} (each prediction retained with probability p_i). If the prediction is dropped, its weight is filled with 0. Then the augmented estimator $\hat{\beta}_i$ obtained from random sampling will satisfy:

$$\mathbb{E}[\hat{\beta}_i] = p_i \hat{\beta}_{old,i}$$

where $\hat{\beta}_{old}$ is the original weight without sampling.

Proof. Assume X is a matrix where the i -th column represents z_i , and Y is the ground truth. Then the ensemble weights $\hat{\beta}_{old}$ can be computed with closed form solution of the objective $\min_{\beta} \|Y - X\beta\|_2$ as:

$$\hat{\beta}_{old} = (X^T X)^{-1} X^T Y.$$

Since $X^T X$ is diagonal, its inverse is also diagonal:

$$(X^T X)^{-1} = \begin{pmatrix} \frac{1}{g_1} & & \\ & \ddots & \\ & & \frac{1}{g_d} \end{pmatrix}.$$

where $g_i = \sum_j x_{ji}^2$ is the sum of squares of the i -th base prediction.

thus

$$\hat{\beta}_{old} = \begin{pmatrix} \frac{1}{g_1} & & \\ & \ddots & \\ & & \frac{1}{g_d} \end{pmatrix} \begin{pmatrix} \sum_i x_{i1} y_i \\ \vdots \\ \sum_i x_{id} y_i \end{pmatrix} = \begin{pmatrix} \frac{\sum_i x_{i1} y_i}{g_1} \\ \vdots \\ \frac{\sum_i x_{id} y_i}{g_d} \end{pmatrix}.$$

Therefore, the i -th component is

$$\hat{\beta}_{old,i} = \frac{\sum_j x_{ji} y_j}{g_i}.$$

Consider independently sampling columns of the design matrix X , retaining each column with probability p_i , resulting in a reduced matrix X' with k columns. The new regression problem is:

$$\min_{\beta} \|Y - X'\beta\|_2^2,$$

with the least squares solution:

$$\hat{\beta} = (X'^T X')^{-1} X'^T Y.$$

Since the columns of X are orthogonal, the columns of X' remain orthogonal after sampling, so $X'^T X'$ is diagonal:

$$X'^T X' = \begin{pmatrix} g_{j_1} & & \\ & \ddots & \\ & & g_{j_k} \end{pmatrix},$$

where j_1, \dots, j_k are the indices of retained columns.

Thus,

$$\hat{\beta} = \begin{pmatrix} \frac{1}{g_{j_1}} & & \\ & \ddots & \\ & & \frac{1}{g_{j_k}} \end{pmatrix} \begin{pmatrix} \sum_i x_{ij_1} y_i \\ \vdots \\ \sum_i x_{ij_k} y_i \end{pmatrix} = \begin{pmatrix} \frac{\sum_i x_{ij_1} y_i}{g_{j_1}} \\ \vdots \\ \frac{\sum_i x_{ij_k} y_i}{g_{j_k}} \end{pmatrix}.$$

We augmented $\hat{\beta}$ such that they have the same dimension, for the dropout column, we fill 0 into $\hat{\beta}_i$, such that their index aligned. On the other hand, if the i -th column is retained, then $\hat{\beta}_i = \hat{\beta}_{old,i}$. In this way, the estimator for the i -th position satisfies:

$$\hat{\beta}_i = \begin{cases} \hat{\beta}_{old,i}, & \text{with probability } p_i, \\ 0, & \text{with probability } 1 - p_i. \end{cases}$$

Thus, its expectation is:

$$\mathbb{E}[\hat{\beta}_i] = p_i \cdot \hat{\beta}_{old,i} + (1 - p_i) \cdot 0 = p_i \hat{\beta}_{old,i}. \quad \square$$

Theorem 2 (Expectation of Average Estimator with Multiple Sampling). Perform N independent random samplings of \mathcal{Z} (each prediction retained with probability p_i), obtaining estimators $\hat{\beta}^{(n)}$ each time. Define the average estimate for the i -th weight as:

$$\bar{\beta}_i^{(N)} = \frac{1}{N} \sum_{n=1}^N \hat{\beta}_i^{(n)}.$$

Then as $N \rightarrow \infty$, we have:

$$\bar{\beta}_i^{(N)} \xrightarrow{\text{a.s.}} p_i \hat{\beta}_{old,i},$$

Proof. From Lemma 1, we know that the expectation of $\hat{\beta}_i^{(n)}$ is:

$$\mathbb{E}[\hat{\beta}_i^{(n)}] = p_i \hat{\beta}_{old,i}.$$

Since each sampling is independent and identically distributed, by the strong law of large numbers, the sample mean almost surely converges to the expected value:

$$\bar{\beta}_i^{(N)} = \frac{1}{N} \sum_{n=1}^N \hat{\beta}_i^{(n)} \xrightarrow{\text{a.s.}} \mathbb{E}[\hat{\beta}_i^{(n)}] = p_i \hat{\beta}_{old,i}, \quad \text{as } N \rightarrow \infty.$$

Thus, for large N , the average weight for the i -th model approaches p_i times the original weight. \square

Algorithm 1: Training a Stacker Model with Dropout and Retain.

Input: The index of the stacker model i , Dropout rate γ_0 , Retain or not, Ensemble size n' , number of folds k , the original training and validation set $\mathcal{D}_{train}, \mathcal{D}_{val}$, the predictive features from last layer $\mathcal{Z}_{train}, \mathcal{Z}_{val}$, the loss function \mathcal{L} .

Output: Prediction of current stacker model.

```
1: y_train  $\leftarrow \mathcal{D}_{train}[:, \text{end}]$ 
2: for  $j = 1$  to  $n'$  do
3:    $\mathcal{L}_j \leftarrow \mathcal{L}(\mathcal{Z}_{train}[:, j], y_{train})$ 
4: end for
5:  $\mathcal{L}_{min} \leftarrow \text{Min}(\mathcal{L}_1, \mathcal{L}_2, \dots, \mathcal{L}_{n'})$ 
6: DropoutRates  $\leftarrow \text{EmptyList}()$ 
7: for  $j = 1$  to  $n'$  do
8:   Append(DropoutRates,  $\frac{\mathcal{L}_{min}}{\mathcal{L}_j} \gamma_0$ )
9: end for
10: folds  $\leftarrow \text{SplitIntoKFolds}(\mathcal{D}_{train}, k)$ .
11: training_prediction  $\leftarrow \text{ZeroArray}(\text{length of } \mathcal{D}_{train})$ .
12: valid_prediction  $\leftarrow \text{ZeroArray}(\text{length of } \mathcal{D}_{val})$ .
13: for  $j = 1$  to  $k$  do
14:   mask  $\leftarrow \text{BernoulliSample}(p = 1 - \text{DropoutRates})$ .
15:   training_indices  $\leftarrow \text{GetAllIndicesExcept}(j, \text{folds})$ .
16:   prediction_indices  $\leftarrow \text{GetIndices}(j, \text{folds})$ .
17:    $\mathcal{D}_{fold\_train} \leftarrow \text{Concatenate}(\mathcal{Z}_{train}[\text{training\_indices}, \text{mask}], \mathcal{D}_{train}[\text{training\_indices}, :])$ . {skip connection}
18:    $S_j \leftarrow \text{TrainModel}(\mathcal{D}_{fold\_train})$ 
19:    $\mathcal{D}_{fold\_predict} \leftarrow \text{Concatenate}(\mathcal{Z}_{train}[\text{prediction\_indices}, \text{mask}], \mathcal{D}_{train}[\text{prediction\_indices}, :])$ .
20:   training_prediction[prediction_indices]  $\leftarrow \text{Predict}(S_j, \mathcal{D}_{fold\_predict})$ . {predict on the prediction fold of the training set}
21:    $\mathcal{D}_{fold\_val} \leftarrow \text{Concatenate}(\mathcal{Z}_{val}[:, \text{mask}], \mathcal{D}_{val})$ .
22:   valid_prediction  $\leftarrow \text{valid\_prediction} + \frac{1}{k} \text{Predict}(S_j, \mathcal{D}_{fold\_val})$ . {predict on the validation set}
23: end for
24: if Retain or not is True then
25:   y_valid  $\leftarrow \mathcal{D}_{valid}[:, \text{end}]$ .
26:    $\mathcal{L}_{val} \leftarrow \mathcal{L}(\text{valid\_prediction}, y_{val})$ .
27:    $\mathcal{L}_{last} \leftarrow \mathcal{L}(\mathcal{Z}_{val}[:, i], y_{val})$ .
28:   if  $\mathcal{L}_{val} > \mathcal{L}_{last}$  then
29:     training_prediction  $\leftarrow \mathcal{Z}_{train}[:, i]$ .
30:     valid_prediction  $\leftarrow \mathcal{Z}_{val}[:, i]$ . {Replace the output with that generated by its predecessor}
31:   end if
32: end if
33: return training_prediction and valid_prediction.
```

Proof of Theorem 1

Proof. We define $p_i = 1 - d_i$, which is the retention probability of each prediction. From Theorem 2, as $N \rightarrow \infty$, the absolute average weight of the i -th prediction is:

$$|\tilde{\beta}_i| = p_i |\beta_i|$$

Then the proportion of $|\tilde{\beta}_1|$ in the sum of all others is:

$$r = \frac{p_1 |\beta_1|}{\sum_{i=1}^d p_i |\beta_i|} = \frac{|\beta_1|}{\sum_{i=1}^d \frac{p_i}{p_1} |\beta_i|} \quad (6)$$

As β_i is constant with the change of γ_0 , we focus on:

$$\frac{p_i}{p_1} = \frac{1 - d_i}{1 - d_1} = \frac{1 - \rho_i \gamma_0}{1 - \gamma_0} = \frac{1 - \rho_i}{1 - \gamma_0} + \rho_i$$

Note that $\rho_i \leq 1$, then $1 - \rho_i \geq 0$, $\frac{p_i}{p_1}$ is monotonically non-decreasing with respect to γ_0 on the interval $[0, 1)$, and strictly increasing if $\rho_i \neq 1$.

As a result, each term in the denominator of Equation 6 is monotonically non-decreasing with respect to γ_0 . Consequently, r is monotonically non-increasing with respect to γ_0 , and strictly decreasing when there exists some $\rho_i \neq 1$.

Thus, the theorem is proved. \square

B Pseudocode of Training a Stacker Model with Dropout and Retain

Algorithm 1 exhibits the pseudocode of training a stacker model with Dropout and Retain in PSEO. First, PSEO will calculate the loss between each predictive feature from the last layer and the training labels (Lines 1-4). It then determines the dropout rate for each predictive feature based on the training losses and γ_0 . Next, PSEO apply k -fold cross-validation to the training set. In each fold, it samples the mask for each predictive feature to retain using a Bernoulli Distribution, and features with a mask of 0 are dropped (Line 14). The stacker model is then trained on the training portion

Algorithm 2: Post-hoc Stacking Optimization Procedure

Input: The search budget \mathcal{B} , the candidate base model pool \mathbb{M} , the ensemble search space \mathcal{X} , the training and validation set $\mathcal{D}_{train}, \mathcal{D}_{val}$.

Output: Best ensemble strategy

- 1: Initialize observations as $D = \emptyset$;
 - 2: Generate predictions of all models in \mathbb{M} on the validation set.
 - 3: **while** budget \mathcal{B} does not exhaust **do**
 - 4: **if** $|D| < 5$ **then**
 - 5: Suggest a random ensemble configuration $\tilde{x} \in \mathcal{X}$.
 - 6: **else**
 - 7: Train a surrogate model on current observations D .
 - 8: Sample configuration candidates from \mathcal{X} and choose the next ensemble configuration by $\tilde{x} \leftarrow \arg \max_{x \in \mathcal{X}} EI(x)$.
 - 9: **end if**
 - 10: Select base model subset \mathbb{K} from \mathbb{M} according to the ensemble size and diversity weight $\tilde{\omega}$ in \tilde{x} .
 - 11: Build a deep stacking ensemble $f_{\tilde{x}}$ with \mathbb{K} .
 - 12: Train the ensemble $f_{\tilde{x}}$ on \mathcal{D}_{train} and evaluate its performance on \mathcal{D}_{val} as \tilde{y} ;
 - 13: Update the observations $D \leftarrow D \cup (\tilde{x}, \tilde{y})$;
 - 14: **end while**
 - 15: **return** the optimal ensemble configuration x^* in D .
-

of the fold and predicts on the rest part (Line 15-20). For the validation set, predictions from all folds are averaged (Line 21-22). Upon completing the training for each fold, if the Retain mechanism is enabled, PSEO calculates the validation loss of the current stacker model compared to the model in the previous layer at the same position (Line 24-27). If the current stacker model performs worse, its outputs will be replaced by those generated by its predecessor (Line 28-30). In the end, the outputs in both the training set and the validation set will be returned (Line 33).

C Pseudocode and Reuse Strategy of PSEO

In this section, we provide the pseudocode of PSEO in Algorithm 2 and the reuse strategy of PSEO.

First, PSEO will collect the predictions of all models in the candidate pool on the validation set (Line 1). Then, while the budget has not been exhausted, the Bayesian optimizer fits a *surrogate model* based on observed configurations D (Line 7). It then suggests the next configuration \tilde{x} to evaluate by maximizing the *acquisition function* $\tilde{x} = \arg \max_{x \in \mathcal{X}} EI(x)$ within the hyperparameter space \mathcal{X} (Line 8). According to hyperparameters in \tilde{x} , PSEO selects the base model subset and builds a stacking ensemble $f_{\tilde{x}}$ (Lines 10-11). After that, PSEO trains and evaluates $f_{\tilde{x}}$ to obtain its performance \tilde{y} and augment the observations by $D = D \cup (\tilde{x}, \tilde{y})$. After exhausting the search budget, the best configuration found in the observations is returned (Line 15). Concretely, PSEO uses the Probabilistic Random Forest (Hutter, Hoos, and Leyton-Brown 2011) as the surrogate of BO and applies the Expected Improvement (EI) as the acquisition function to estimate the performance improvement

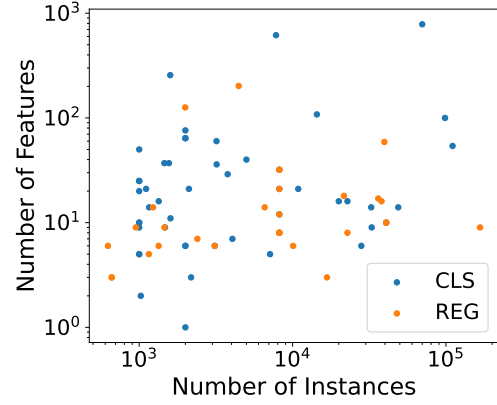


Figure 6: Datasets by Data Dimensions

given an unseen configuration.

By default, PSEO saves to disk each stacking ensemble constructed during the optimization process. If a new ensemble configuration $f_{\tilde{x}}$ shares the same base models subset, dropout rate, and retain settings as a previously trained ensemble $f_{x'}$, the cached results can be reused to avoid redundant computation. Specifically, if $f_{\tilde{x}}$ has more stacking layers than $f_{x'}$, training can resume by stacking additional layers on top of $f_{x'}$. Conversely, if the number of layers in $f_{\tilde{x}}$ is fewer than or equal to that in $f_{x'}$, only the blender model corresponding to the target layer needs to be retrained on top of $f_{x'}$'s intermediate output.

D Dataset Details

In Tables 8 and 9, we provide the details of the datasets used in our experiment. The datasets are selected according to the following list of criteria:

- **Representative of real-world.** We limit artificial problems, including only a small selection of such problems, either based on their widespread use (e.g., kr-vs-kp) or because they pose difficult problems.
- **Diversity in task type.** We include 50 classification datasets, 12 of which are multi-class datasets. We also include 30 regression datasets, which many studies tend to overlook in their experiments (Poduval et al. 2024; Erickson et al. 2020).
- **Diversity in data Dimensions.** We aim to comprehensively cover datasets ranging from small to large scales in both feature and sample dimensions. As shown in Figure 6, the number of features ranges from 1 to 784, and the number of instances ranges from 0.6k to 166k.
- **Diversity in the problem domains.** We do not want the benchmark to skew towards any application domain in particular. Therefore, various domains like software quality problems (jm1, kc1, pc1, pc3, pc4), handwritten digit recognition (mfeat-morphological(1), mnist_784), Aerospace (delta_aileron), Business (ama-

Type of Classifier	# λ	cat (cond)	cont (cond)
AdaBoost	4	1 (-)	3 (-)
Random forest	5	2 (-)	3 (-)
Extra trees	5	2 (-)	3 (-)
Gradient boosting	7	1 (-)	6 (-)
KNN	2	1 (-)	1 (-)
LDA	4	1 (-)	3 (1)
QDA	1	-	1 (-)
Logistic regression	4	2 (-)	2 (-)
Liblinear SVC	5	2 (2)	3 (-)
LibSVM SVC	7	2 (2)	5 (-)
LightGBM	6	-	6 (-)
Type of Regressor	# λ	cat (cond)	cont (cond)
AdaBoost	4	1 (-)	3 (-)
Random forest	5	2 (-)	3 (-)
Extra trees	5	2 (-)	3 (-)
Gradient boosting	7	1 (-)	6 (-)
KNN	2	1 (-)	1 (-)
Lasso	3	-	3 (-)
Ridge	4	1 (-)	3 (-)
Liblinear SVC	5	2 (2)	3 (-)
LibSVM SVC	8	3 (3)	5 (-)
LightGBM	6	-	6 (-)

Table 5: Search space for ML algorithms. We distinguish categorical (cat) hyperparameters from numerical (cont) ones. The numbers in the brackets are conditional hyperparameters.

zon_employee), computer performance (puma32H, cpu_small, cpu_act, puma8NH), and so forth.

- **Freely available.** All the datasets are collected from OpenML (Vanschoren et al. 2014), and we provide the OpenML ID as the identification of the dataset.

E Search Space of CASH

The search space for algorithms and feature engineering operators is presented in Tables 5 and 6, respectively.

F Implementation Details

The Bayesian optimization surrogate is implemented using OpenBox 0.8.1 (Li et al. 2021; Jiang et al. 2024a), an open-source toolkit designed for black-box optimization tasks. We adhered to the open-source versions or the methodologies outlined in the original papers for all other baseline implementations. For EO, the ensemble size is set to 12. For Autostacker, the maximum number of layers and the maximum number of nodes per layer are 5 and 3, the population size is set to 200. In the case of OptDivBO, the parameter of τ is 0.2. For all ensemble selection designs, the ensemble size is fixed at 25, with ensemble weights trained using the base models’ predictions on the validation data. For all stacking designs, the number of folds for cross-validation during training is set to 5. All the experiments are conducted with 24 CPU cores and 80G memory.

To fully and fairly utilize all non-test data, ensemble

Type of Operator	# λ	cat (cond)	cont (cond)
Minmax	0	-	-
Normalizer	0	-	-
Quantile	2	1 (-)	1 (-)
Robust	2	-	2 (-)
Standard	0	-	-
Cross features	# λ	cat (cond)	cont (cond)
Fast ICA	4	3 (1)	1 (1)
Feature agglomeration	4	3 (2)	1 (-)
Kernel PCA	5	1 (1)	4 (3)
Rand. kitchen sinks	2	-	2 (-)
LDA decomposer	1	1 (-)	-
Nystroem sampler	5	1 (1)	4 (3)
PCA	2	1 (-)	1 (-)
Polynomial	2	1 (-)	1 (-)
Random trees embed.	5	1 (-)	4 (-)
SVD	1	-	1 (-)
Select percentile	2	1 (-)	1 (-)
Select generic univariate	3	2 (-)	1 (-)
Extra trees preprocessing	5	2 (-)	3 (-)
Linear SVM preprocessing	5	3 (3)	2 (-)

Table 6: Search space of feature engineering operators.

selection-based methods determine ensemble weights on the validation set. After that, the base models are refitted using both the training and validation sets. Fixed-strategy stacking methods concatenate the training and validation sets for cross-validation training. Optimized stacking methods (Autostacker, AutoGluon, and PSEO) first perform cross-validation on the training set, evaluate performance on the validation set, and finally refit the optimal ensemble using both training and validation sets.

G Effectiveness of Deep Stacking Structure

To assess the effectiveness and tuning potential of the deep stacking framework of PSEO, this experiment compares the performance of different values for four hyperparameters of deep stacking (using a fixed subset of 30 base models selected with a diversity weight of 0.3). For the dropout rate, values of 0, 0.1, 0.2, 0.3, and 0.4 are tested; For the number of layers, values of 1, 2, 3, 4, and 5 are considered. For the blender model, ensemble selection (ES), Linear, and LightGBM (LGB) are tested. And “retain or not” takes True or False Due to the vast configuration space, we conducted separate experiments for each hyperparameter instead of a full grid search. Specifically, for each hyperparameter, we held the other hyperparameters at their median values from the set of possible values, then iterated over all values for the target hyperparameter to construct stacking ensembles. The optimal value (OPT) was selected based on validation set performance. This optimal configuration was then compared to all fixed-value ensembles for the hyperparameter on the test set, with the average rank calculated across 80 datasets. Notably, when fixing the Blender model, we used Linear, and when fixing the Retain strategy, we set it to True.

Figure 1 shows the average test rank across each hyperparameter’s values, where each hyperparameter exper-

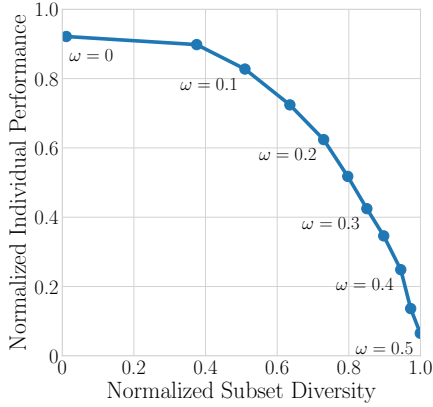


Figure 7: Relationship between normalized average individual performance and normalized diversity among the base model subset across 80 datasets for varying diversity weights. We execute base model subset selection with 11 diversity weights ranging from 0 to 0.5 in increments of 0.05. For each dataset, the average performance of 30 selected base models with different diversity weights was calculated and normalized using min-max scaling from 0 to 1. The subset diversity was assessed and normalized in the same way.

iment was conducted independently and compared separately. From this analysis, we observe that 1) for the three hyperparameters—dropout rate, number of layers, and blender model—no specific value consistently outperforms others. This is evident from the fact that the average rank differences between the top two fixed value schemes are only 0.03, 0.10, and 0.18, excluding Opt. Therefore, the optimal values for these hyperparameters are highly task-dependent. Correspondingly, tuning these parameters significantly improves performance, as OPT surpasses the best fixed scheme by 0.83, 0.73, and 0.61 in average rank, far exceeding the differences between fixed values. 2) For the retain or not hyperparameter, "True" already shows a clear advantage over "False", with average ranks of 1.5 and 1.85, respectively. However, selecting values based on the validation set can further improve the rank to 1.3. In summary, all four hyperparameters of the deep stacking framework merit tuning to identify task-specific optimal values.

H Trade-off Between Individual Model Performance and Inter-model Diversity

In this experiment, we aim to validate the base model selection algorithm of PSEO by exploring the impact of varying diversity weights. By setting the ensemble size to 30 and adjusting the diversity weights, ranging from 0 to 0.5 in increments of 0.05, we investigate the trade-off between individual model performance and subset diversity.

Specifically, for each diversity weight value, we calculated the average individual performance of the selected base models, defined as the average of their metrics on the task. For classification tasks, this metric is *accuracy*, and for regression tasks, it is the negative of

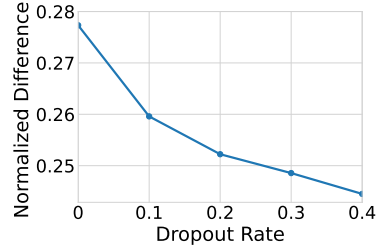


Figure 8: Normalized difference between training and test performance changing with dropout rate.

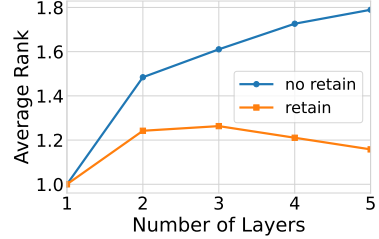


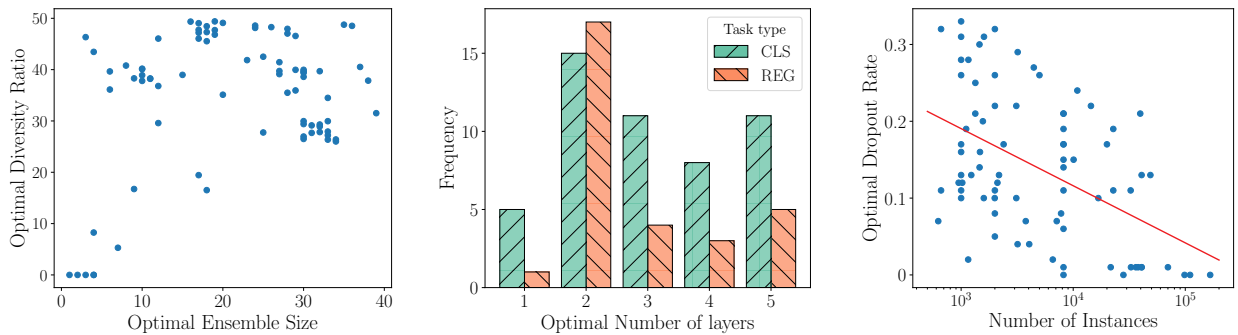
Figure 9: Average rank of output with(out) Retain.

mean squared error (MSE). A higher value indicates better individual performance. Similarly, we assessed the diversity within the selected base models subset by computing the average pair-wise diversity, derived from the Equation 2. We use its negative to describe diversity. A higher value indicates greater diversity.

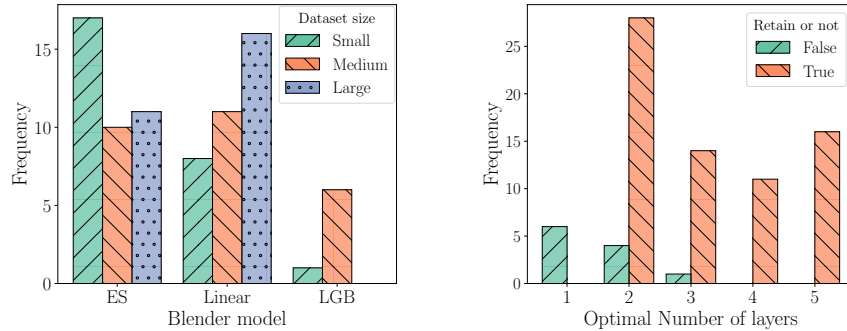
To synthesize results across all tasks, we apply min-max normalization to both individual performance and subset diversity for each dataset across the 11 diversity weight values, scaling them to a range of 0 to 1. Subsequently, we average these normalized results over 80 tasks and show the results in Figure 7. We observed that: 1) The 11 points, from left to right, represent the increasing diversity weights from the smallest to the largest value. Correspondingly, the individual performance of the selected base model subset decreases, while diversity increases, demonstrating a clear trade-off. 2) The trade-off curve is convex towards the upper right. This indicates that as the diversity weight increases, diversity gains diminish compared to the loss in individual performance. Initially, small increases in dropout improve diversity without significantly sacrificing performance. However, further increases lead to greater performance losses with smaller diversity gains.

I Effectiveness of Dropout Mechanism

To highlight the effect of Dropout on the overfitting issue, Figure 8 shows the average normalized difference between training and test performance with dropout rate changing from 0 to 0.4 across 80 datasets. Specifically, the normalized difference is the ratio of the absolute value of the difference between the training loss and test loss to the absolute value of the training loss: $|\mathcal{L}_{train} - \mathcal{L}_{test}|/|\mathcal{L}_{train}|$. We observe that as the dropout rate increases, the gap between the



(a) Optimal base model selection strategy across all tasks. (b) Optimal number of layers for different task types. (c) Optimal dropout ratios for tasks with different dataset sizes.



(d) Optimal blender model for tasks with different dataset sizes.

(e) Optimal number of layers with optimal retain or not parameter.

Figure 10: Optimal Configuration Analysis.

	Single-Best	w/o Retain	w/o Dropout	PSEO
CLS	3.24	2.04	1.84	1.46
REG	3.67	2.30	2.27	1.70
ALL	3.40	2.14	2.00	1.55

Table 7: Average test rank.

training and test performance gradually narrows, indicating a reduction in overfitting.

J Effectiveness of Retain Mechanism

To highlight the effect of predictive feature quality on ensemble performance, Figure 9 uses a linear model as the blender and shows the average test rank of stacking with and without the Retain mechanism, as stacking depth increases. The results indicate that the Retain mechanism performs increasingly better, widening the gap over the baseline.

K Critical Difference Diagram

Figure 11(a) shows the results of the Conover post hoc test using critical difference plots, whereby a horizontal bar connects methods that are not significantly different.

L Ablation Study

In this section, we present the effects of two mechanisms in PSEO via an ablation study in Table 7. We evaluate: 1) Single-Best; 2) w/o Retain: PSEO without the Retain mechanism; 3) w/o Dropout: PSEO without the Dropout mechanism; 4) PSEO. We further calculate the improvement rates of each method over Single-Best for each dataset. The average improvements of w/o Retain, w/o Dropout, and PSEO are 9.8%, 7.7%, and 11.0%, respectively. First, removing either mechanism leads to lower average rankings compared to the full PSEO, and also results in reduced improvement over the Single-Best baseline. Secondly, the ranking of w/o Retain is lower than that of w/o Dropout, but its improvement rate over Single-Best is higher. This suggests that the Dropout can elevate the upper bound of stacking performance on datasets prone to overfitting, while the Retain mechanism maintains the lower bound for most datasets. To summarize, the two mechanisms of PSEO show performance improvement. It indicates that the deep stacking framework of PSEO is a reasonable design that provides a flexible framework adaptable to various tasks, along with optional strategies for addressing specific issues.

M Optimal Configuration Analysis

In this section, we analyze the optimal ensemble strategies identified by PSEO across 80 ML tasks, aiming to provide

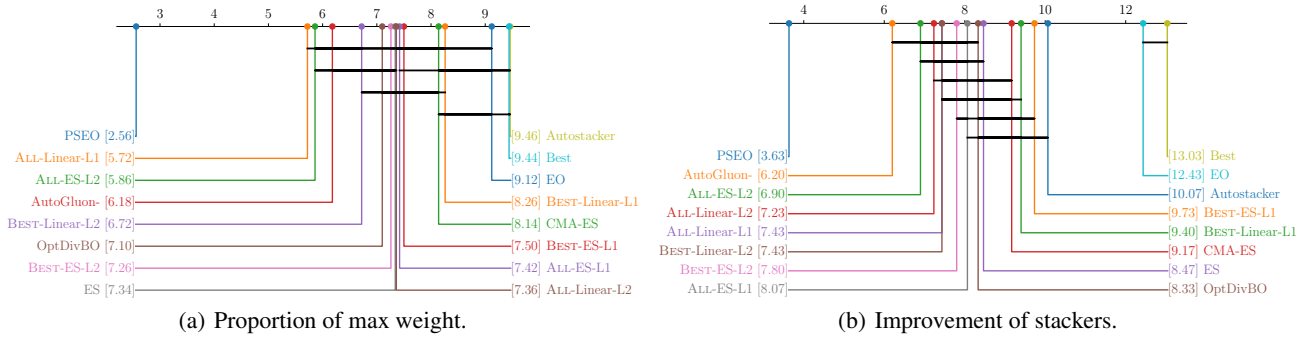


Figure 11: Effectiveness of Dropout and Retain mechanisms.

insights for designing post-hoc ensemble strategies tailored to different tasks. Figure 10 presents the results of five analyses, each of which will be detailed individually below.

1) We extracted the base model selection strategies from the optimal ensembles across 80 tasks to examine the relationship between optimal ensemble size and optimal diversity weight. The scatter plot is shown in Figure 10(a). We observe that **most optimal configurations have a high diversity weight** (greater than 0.25), indicating that diversity can enhance ensemble performance. Additionally, the absence of points in the lower right corner suggests that **large ensemble sizes coupled with low diversity weights are typically not optimal**, as this situation may lead to overfitting.

2) For the number of stacking layers, we plotted the distribution of optimal ensemble stacking layers separately for classification and regression tasks, as shown in Figure 10(b). We observe that **the most common optimal ensemble stacking layer number is two**, particularly for regression tasks, with 17 out of 30 tasks having an optimal stacking of two layers, while the frequency for other layer counts does not exceed 5. In contrast, for classification tasks, the frequency of optimal stacking layers ranging from three to five is relatively closer to that of two. **This suggests that classification tasks have greater potential for deeper stacking, whereas regression tasks may experience instability and suboptimal performance with higher stacking layers.**

3) Regarding the choice of dropout rate, we plotted the relationship between the optimal dropout rate and the number of instances in the dataset for 80 tasks, as shown in Figure 10(c). The red line represents the fitted linear trend. We can observe that, generally, as the dataset size increases, the optimal dropout rate tends to decrease. **This indicates that smaller datasets require the Dropout mechanism more**, as overfitting is more likely to occur in such tasks.

4) For the blender model, we sorted the 80 datasets by the number of instances and divided them into three categories: small datasets (less than 1.6k), medium datasets (2k to 8k), and large datasets (greater than 10k). We then plotted the distribution of optimal Blender models for each category, as shown in Figure 10(d). We observe that **the LGB model is generally not the optimal choice**, with only 7 out of 80 tasks selecting it as the best blender model. **ES and Linear perform similarly overall, with ES showing a clear ad-**

vantage on smaller datasets. As the dataset size increases, the performance of the Linear tends to improve.

5) Regarding the Retain mechanism, we examine the relationship between whether Retain is used in the optimal configuration and the number of stacking layers. Figure 10(e) shows the distribution of the optimal number of stacking layers where Retain is set to True and False, respectively. We can conclude that the **Retain mechanism is recommended to be enabled**, as it is set to True in the optimal configuration for 69 out of 80 tasks. Additionally, **to achieve better ensemble performance with higher stacking layers, Retain is essential**, because when the optimal number of stacking layers exceeds one, Retain is almost always True.

N Test Performance Per Dataset Per Method

This section provides the exact performance of each method per dataset. Tables 10, 11, and 12 present the test errors for all methods across 50 classification tasks, where test error equals $1 - \text{accuracy}$. Tables 13, 14, and 15 show the test errors for all methods across 30 regression tasks, where test error equals the *mean squared error* (MSE).

O Detailed Information about Reproducibility Checklist

- 1. General Paper Structure
 - 1.1. Includes a conceptual outline and/or pseudocode description of AI methods introduced. [yes]. See Algorithm 1 in Appendix B and Algorithm 2 in Appendix C.
 - 1.2. Clearly delineates statements that are opinions, hypothesis, and speculation from objective facts and results. [yes].
 - 1.3. Provides well-marked pedagogical references for less-familiar readers to gain background necessary to replicate the paper. [yes]. We have provided references to foundational and cutting-edge articles in the field, along with sources for all experimental data.
- 2. Theoretical Contributions
 - 2.1. Does this paper make theoretical contributions?

- [yes]. See Theorem 1 and Theorem 2.
- 2.2. All assumptions and restrictions are stated clearly and formally. [yes]. See Theorem 1, Theorem 2 and Section 3.2.
 - 2.3. All novel claims are stated formally (e.g., in theorem statements). [yes]. See Theorem 1 and Theorem 2.
 - 2.4. Proofs of all novel claims are included. [yes]. See the proof in Appendix A.
 - 2.5. Proof sketches or intuitions are given for complex and/or novel results. [yes]. See the proof sketch in Appendix A.
 - 2.6. Appropriate citations to theoretical tools used are given. [yes].
 - 2.7. All theoretical claims are demonstrated empirically to hold. [yes].
 - 2.8. All experimental code used to eliminate or disprove claims is included. [yes]. See the code in “PSEO_code/examples/benchmark_ana_dropout.py”.
- 3. Dataset Usage
 - 3.1. Does this paper rely on one or more datasets? [yes]. We rely on 80 public datasets in our experiment in Section 4.
 - 3.2. A motivation is given for why the experiments are conducted on the selected datasets. [yes]. We provide the list of criteria for selecting datasets in Appendix D.
 - 3.3. All novel datasets introduced in this paper are included in a data appendix. [NA]. We haven’t introduced novel datasets.
 - 3.4. All novel datasets introduced in this paper will be made publicly available upon publication of the paper with a license that allows free usage for research purposes. [NA]. We haven’t introduced novel datasets.
 - 3.5. All datasets drawn from the existing literature (potentially including authors’ own previously published work) are accompanied by appropriate citations. [yes]. All the datasets are collected from OpenML (Vanschoren et al. 2014), and we provide the OpenML ID as the identification of the dataset.
 - 3.6. All datasets that are not publicly available are described in detail, with explanation why publicly available alternatives are not scientifically satisfying. [NA]. All the datasets are publicly available in OpenML.
 - 4. Computational Experiments
 - 4.1. Does this paper include computational experiments. [yes]. See Section 4.
 - 4.2. This paper states the number and range of values tried per (hyper-) parameter during development of the paper, along with the criterion used for selecting the final parameter setting. [yes]. We decide the hyperparameters through tuning.
 - 4.3. Any code required for pre-processing data is included in the appendix. [yes]. See the code in “PSEO_code/examples/benchmark_pseo.py” file.
 - 4.4. All source code required for conducting and analyzing the experiments is included in a code appendix. [yes]. See the code in “PSEO_code/examples/benchmark_pseo.py” and “PSEO_code/examples/benchmark_ana_rank.py”.
 - 4.5. All source code required for conducting and analyzing the experiments will be made publicly available upon publication of the paper with a license that allows free usage for research purposes. [yes]. We will open-source the code in GitHub upon publication.
 - 4.6. All source code implementing new methods have comments detailing the implementation, with references to the paper where each step comes from. [yes]. See the code in “PSEO_code/pseo” directory.
 - 4.7. If an algorithm depends on randomness, then the method used for setting seeds is described. [NA].
 - 4.8. This paper specifies the computing infrastructure used for running experiments (hardware and software), including GPU/CPU models; amount of memory; operating system; names and versions of relevant software libraries and frameworks. [yes]. See Appendix F.
 - 4.9. This paper formally describes evaluation metrics used and explains the motivation for choosing these metrics. See Section 4.1.
 - 4.10. This paper states the number of algorithm runs used to compute each reported result. [yes].
 - 4.11. Analysis of experiments goes beyond single dimensional summaries of performance (e.g., average; median) to include measures of variation, confidence, or other distributional information. [yes]. See Figure 5 and Section 4.4.
 - 4.12. The significance of any improvement or decrease in performance is judged using appropriate statistical tests (e.g., Wilcoxon signed-rank). [yes]. See Section 4.5.
 - 4.13. This paper lists all final (hyper-)parameters used for each model/algorithm in the paper’s experiments. [yes]. See Appendix F.

Datasets	Task Type	OpenML ID	Classes	Samples	Features
fri_c0_1000_5	CLS	609	2	1000	5
fri_c2_1000_5	CLS	599	2	1000	5
fri_c4_1000_10	CLS	623	2	1000	10
fri_c1_1000_50	CLS	583	2	1000	50
credit	CLS	46116	2	1000	9
fri_c3_1000_10	CLS	608	2	1000	10
fri_c0_1000_25	CLS	598	2	1000	25
credit-g	CLS	31	2	1000	20
fri_c3_1000_25	CLS	586	2	1000	25
rmftsa_sleepdata(1)	CLS	679	4	1024	2
pc1	CLS	1068	2	1109	21
colleges_aaup	CLS	488	2	1161	14
analcata_data_halloffame	CLS	454	2	1340	16
pc4	CLS	1049	2	1458	37
cmc	CLS	23	3	1473	9
pc3	CLS	1050	2	1563	37
semeion	CLS	1501	10	1593	256
winequality_red	CLS	42184	6	1599	11
mfeat-morphological(1)	CLS	18	10	2000	6
mfeat-morphological(2)	CLS	962	2	2000	6
mfeat-karhunen(2)	CLS	1020	2	2000	64
mfeat-karhunen(1)	CLS	16	10	2000	64
mfeat-fourier(1)	CLS	14	10	2000	76
balloon	CLS	512	2	2001	1
kc1	CLS	1067	2	2109	21
quake	CLS	209	2	2178	3
space_ga	CLS	507	2	3107	6
splice	CLS	46	3	3190	60
kr-vs-kp	CLS	3	2	3196	36
hypothyroid(2)	CLS	1000	2	3772	29
analcata_data_supreme	CLS	504	2	4052	7
waveform-5000(2)	CLS	979	2	5000	40
delta_ailerons	CLS	803	2	7129	5
isolet	CLS	300	26	7797	617
puma32H	CLS	308	2	8192	32
cpu_small	CLS	227	2	8192	12
puma8NH	CLS	225	2	8192	8
cpu_act	CLS	197	2	8192	21
jm1	CLS	1053	2	10885	21
sylva_prior	CLS	1040	2	14395	108
letter(2)	CLS	977	2	20000	16
house_16H	CLS	574	2	22784	16
kropt	CLS	184	18	28056	6
adult-census	CLS	1119	2	32561	14
amazon_employee	CLS	4135	2	32769	9
mv	CLS	344	2	40768	10
adult	CLS	179	2	48842	14
mnist_784	CLS	554	10	70000	784
vehicle_sensIT	CLS	357	2	98528	100
covertype	CLS	180	7	110393	54

Table 8: Basic information of classification dataset.

Datasets	Task Type	OpenML ID	Samples	Features
strikes	REG	549	625	6
disclosure_x_noise	REG	704	662	3
disclosure_z	REG	699	662	3
stock	REG	223	950	9
socmob	REG	541	1156	5
Moneyball	REG	41021	1232	14
insurance	REG	43463	1338	6
weather_izmir	REG	42369	1461	9
us_crime	REG	42730	1994	126
debutanizer	REG	23516	2394	7
space_ga	REG	507	3107	6
mtp	REG	405	4450	202
wind	REG	503	6574	14
bank32nh	REG	558	8192	32
bank8FM	REG	572	8192	8
cpu_act	REG	197	8192	21
cpu_small	REG	227	8192	12
kin8nm	REG	189	8192	8
puma32H	REG	308	8192	32
puma8NH	REG	225	8192	8
sulfur	REG	23515	10081	6
rainfall_bangladesh	REG	41539	16755	3
kc_house_data	REG	42079	21613	18
house_8L	REG	218	22784	8
NewFuelCar	REG	41506	36203	17
electricity_prices_ICON	REG	1168	38014	16
OnlineNewsPopularity	REG	42724	39644	59
2dplanes	REG	215	40768	10
mv	REG	344	40768	10
black_friday	REG	41540	166821	9

Table 9: Basic information of regression dataset.

Datasets	Single-Best	EO	Autostacker	OptDivBO	ES	CMAES	ALL-ES-L1
fri_c0_1000_5	9.5000	10.0000	10.0000	10.0000	10.5000	9.5000	9.0000
fri_c2_1000_5	6.5000	8.0000	7.5000	6.0000	6.0000	5.5000	6.5000
fri_c4_1000_10	4.5000	7.0000	12.0000	8.5000	7.5000	4.5000	9.5000
fri_c1_1000_50	7.0000	7.5000	4.5000	5.0000	6.0000	7.0000	5.5000
credit	28.5000	28.5000	29.5000	28.0000	28.0000	28.5000	25.5000
fri_c3_1000_10	13.0000	<u>9.0000</u>	11.5000	<u>9.0000</u>	10.5000	11.0000	10.5000
fri_c0_1000_25	11.0000	11.5000	9.0000	8.5000	10.0000	11.0000	9.0000
credit-g	24.5000	22.0000	22.0000	23.0000	19.5000	21.0000	20.5000
fri_c3_1000_25	6.5000	6.0000	3.0000	6.5000	6.5000	6.5000	8.0000
rmftsa_sleepdata(1)	50.2439	46.8293	53.1707	46.3415	48.2927	48.7805	46.8293
pc1	<u>5.8559</u>	6.3063	7.2072	6.7568	<u>5.8559</u>	<u>5.8559</u>	6.7568
colleges_aaup	1.2876	0.8584	0.8584	0.8584	1.2876	1.2876	1.2876
analcatadata_halloffame	4.8507	3.7313	5.2239	4.4776	4.8507	4.8507	4.4776
pc4	7.8767	8.2192	11.3014	11.6438	9.9315	7.8767	9.5890
cmc	42.7119	48.8136	43.3898	42.3729	<u>41.6949</u>	42.7119	42.0339
pc3	10.2236	10.2236	10.5431	10.5431	<u>10.2236</u>	10.2236	10.2236
semeion	<u>3.7618</u>	<u>3.7618</u>	4.7022	4.3887	<u>3.7618</u>	5.0157	4.7022
winequality_red	29.0625	31.5625	30.6250	31.2500	28.7500	27.8125	29.3750
mfeat-morphological(1)	26.0000	27.0000	21.5000	21.0000	25.5000	26.0000	25.5000
mfeat-morphological(2)	0.2500						
mfeat-karhunen(2)	0.5000	0.2500	0.2500	0.2500	0.0000	0.5000	0.0000
mfeat-karhunen(1)	<u>2.2500</u>	<u>2.2500</u>	2.5000	<u>2.2500</u>	3.0000	<u>2.2500</u>	3.2500
mfeat-fourier(1)	17.5000	16.5000	15.7500	14.5000	17.0000	17.5000	17.5000
balloon	14.2145						
kc1	13.5071	14.4550	12.5592	12.5592	12.0853	13.5071	12.3223
quake	49.3119	46.1009	49.5413	48.3945	48.6239	45.6422	<u>45.4128</u>
space_ga	13.8264	17.2026	12.5402	12.5402	13.3441	14.1479	12.0579
splice	3.9185	3.9185	3.6050	4.2320	3.4483	3.9185	3.7618
kr-vs-kp	0.6250	0.6250	0.7812	0.7812	0.4687	0.6250	0.6250
hypothyroid(2)	0.2649						
analcatadata_supreme	0.6165	0.4932	0.7398	0.6165	0.4932	0.6165	0.7398
waveform-5000(2)	10.9000	9.9000	18.3000	9.5000	10.1000	9.6000	9.1000
delta_ailérons	6.0309	5.7504	6.0309	<u>5.8906</u>	6.2412	6.0309	5.9607
isolet	3.0769	3.1410	2.9487	<u>2.8205</u>	3.0769	3.0128	3.0769
puma32H	8.6028	12.3246	8.0537	8.2977	9.3350	8.7248	8.7858
cpu_small	7.3826	7.0775	7.7486	7.9317	7.5656	7.5046	7.5046
puma8NH	17.2056	17.9988	16.7175	17.1446	16.7175	17.5717	16.9616
cpu_act	6.8944	6.4674	6.5284	6.4674	6.3453	6.8944	6.5284
jm1	18.1442	18.0524	17.9146	18.1442	17.2715	17.7308	17.8227
sylva_prior	0.5210	0.4515	0.5210	0.4168	0.5210	0.5210	0.5210
letter(2)	0.1000	0.0750	0.0500	<u>0.0250</u>	<u>0.0250</u>	0.0500	<u>0.0250</u>
house_16H	10.4016	10.0505	10.0066	9.6774	9.7652	10.0944	9.8310
kropt	<u>7.2701</u>	12.0991	9.1411	8.5709	7.8582	7.2880	14.9679
adult-census	13.2197	15.7070	13.0355	13.1890	13.3272	<u>12.8512</u>	12.9894
amazon_employee	4.8062	5.2487	4.6689	4.6842	4.6689	4.8062	4.8062
mv	0.0491	0.1104	0.0858	0.0613	0.1104	0.0491	0.0368
adult	13.9114	14.4846	13.9114	14.0035	13.8704	13.7271	13.9728
mnist_784	1.8286	1.8286	2.0500	1.3714	1.6214	1.5000	1.5357
vehicle_sensIT	12.9605	12.9605	12.5444	<u>12.3566</u>	12.9402	12.9554	12.9301
coverttype	11.5766	11.1871	9.1852	<u>9.1308</u>	10.1363	9.9733	11.5766

Table 10: Test Error(%) - CLS(Part I): The test score for each method. The best methods per dataset are shown in bold, while the second-best methods are underlined.

Datasets	ALL-ES-L2	ALL-Linear-L1	ALL-Linear-L2	BEST-ES-L1	BEST-ES-L2	BEST-Linear-L1
fri_c0_1000_5	9.0000	8.5000	9.5000	12.0000	10.5000	12.0000
fri_c2_1000_5	6.0000	6.0000	6.5000	6.5000	7.0000	7.5000
fri_c4_1000_10	9.0000	5.5000	9.5000	8.5000	9.5000	9.5000
fri_c1_1000_50	<u>3.5000</u>	3.0000	4.5000	4.5000	4.0000	5.0000
credit	27.5000	<u>26.5000</u>	31.5000	27.0000	29.5000	28.5000
fri_c3_1000_10	7.5000	<u>9.0000</u>	11.5000	12.0000	10.0000	10.5000
fri_c0_1000_25	9.0000	8.0000	8.0000	9.0000	9.0000	8.5000
credit-g	20.0000	21.0000	21.0000	20.5000	24.0000	20.0000
fri_c3_1000_25	<u>1.5000</u>	4.5000	4.5000	6.5000	5.5000	5.5000
rmftsa_sleepdata(1)	47.8049	45.3659	49.2683	46.8293	47.8049	46.8293
pc1	8.5586	7.6577	7.2072	6.3063	<u>5.8559</u>	6.7568
colleges_aaup	0.8584	1.2876	1.2876	1.2876	1.2876	1.7167
analcata_data_halloffame	4.8507	<u>4.1045</u>	4.4776	4.8507	4.4776	4.8507
pc4	9.5890	10.6164	9.5890	9.2466	9.5890	9.5890
cmc	43.7288	43.3898	46.7797	42.0339	44.0678	40.0000
pc3	10.5431	10.5431	9.9042	10.2236	<u>9.5847</u>	10.5431
semeion	4.3887	4.7022	4.3887	4.0752	4.3887	3.4483
winequality_red	30.0000	32.8125	33.4375	<u>28.1250</u>	31.2500	29.0625
mfeat-morphological(1)	<u>19.2500</u>	20.5000	22.7500	25.7500	21.2500	21.2500
mfeat-morphological(2)	0.2500	0.2500	0.2500	0.2500	0.2500	0.2500
mfeat-karhunen(2)	0.2500	0.2500	0.2500	0.2500	0.0000	0.2500
mfeat-karhunen(1)	2.5000	<u>2.2500</u>	2.7500	<u>2.2500</u>	<u>2.2500</u>	3.0000
mfeat-fourier(1)	17.5000	<u>12.2500</u>	13.5000	17.5000	17.5000	12.7500
balloon	15.2120	14.2145	14.2145	14.2145	14.2145	14.2145
kc1	12.0853	12.0853	12.5592	12.0853	12.3223	12.3223
quake	47.7064	49.3119	<u>45.4128</u>	44.7248	49.3119	<u>45.4128</u>
space_ga	12.8617	12.2186	11.5756	12.7010	12.7010	13.0225
splice	<u>3.2915</u>	2.8213	<u>3.2915</u>	3.9185	3.7618	3.4483
kr-vs-kp	0.6250	0.6250	0.6250	0.6250	0.4687	0.6250
hypothyroid(2)	0.2649	0.2649	0.2649	0.2649	0.2649	0.3974
analcata_data_supreme	0.7398	0.7398	0.7398	0.7398	0.7398	0.7398
waveform-5000(2)	9.1000	10.1000	9.5000	9.9000	9.9000	10.1000
delta_ailerons	5.9607	6.1010	6.3815	<u>5.8906</u>	5.9607	5.9607
isolet	2.9487	2.9487	<u>2.6923</u>	<u>3.0128</u>	2.6282	3.2692
puma32H	7.8707	7.1385	7.8707	8.4198	7.8096	8.9689
cpu_small	7.4436	7.5046	7.5046	7.3215	7.6876	7.5656
puma8NH	<u>16.6565</u>	16.4735	17.2056	16.9005	16.8395	16.8395
cpu_act	6.2843	5.7962	6.1013	6.5894	6.1623	6.7724
jm1	17.5011	17.0877	18.0983	16.8581	17.8227	<u>17.0418</u>
sylva_prior	0.3821	0.3821	0.4515	0.5557	0.4863	0.4515
letter(2)	<u>0.0250</u>	0.0500	<u>0.0250</u>	0.0500	0.0500	0.0000
house_16H	9.9408	9.5458	9.9627	9.9408	9.9846	9.7871
kropt	8.3393	11.0478	8.7847	14.8076	10.4419	13.5424
adult-census	12.8819	13.0508	13.0815	13.1122	13.0355	13.2044
amazon_employee	4.6384	4.5468	4.7910	4.8520	4.7147	4.7605
mv	0.0368	0.1226	<u>0.0245</u>	0.0858	0.0368	0.0736
adult	13.9625	13.8806	14.6279	13.9318	13.8806	14.0035
mnist_784	1.4071	<u>1.3643</u>	1.4000	1.5857	1.5643	1.5929
vehicle_sensIT	12.4480	12.8438	12.4023	12.8540	12.5647	13.1534
covertype	11.5766	12.7678	11.4362	11.5766	11.5766	9.6562

Table 11: Test Error(%) - CLS(Part II): The test score for each method. The best methods per dataset are shown in bold, while the second-best methods are underlined.

Datasets	BEST-Linear-L2	AutoGluon-	PSEO
fri_c0_1000_5	11.0000	9.0000	8.5000
fri_c2_1000_5	6.5000	6.3595	5.5000
fri_c4_1000_10	8.0000	9.3736	7.5000
fri_c1_1000_50	<u>3.5000</u>	5.4807	<u>3.5000</u>
credit	29.0000	26.9174	27.5000
fri_c3_1000_10	11.0000	9.6385	<u>9.0000</u>
fri_c0_1000_25	9.0000	9.0000	8.5000
credit-g	22.5000	19.9686	19.5000
fri_c3_1000_25	3.5000	0.0000	4.0000
rmftsa_sleepdata(1)	48.2927	47.7064	<u>45.8537</u>
pc1	5.4054	8.3585	<u>5.8559</u>
colleges_aaup	1.2876	1.2184	0.8584
analcata_halloffame	4.8507	4.4593	4.4776
pc4	9.5890	9.5890	9.5890
cmc	42.3729	41.9174	42.0339
pc3	8.9457	10.4732	9.9042
semeion	4.0752	4.6679	<u>3.7618</u>
winequality_red	31.5625	29.3248	29.0625
mfeat-morphological(1)	20.2500	19.1617	20.5000
mfeat-morphological(2)	0.2500	0.2500	0.2500
mfeat-karhunen(2)	0.0000	0.0000	0.2500
mfeat-karhunen(1)	2.5000	3.0563	2.0000
mfeat-fourier(1)	11.7500	17.5000	<u>12.2500</u>
balloon	14.2145	15.1321	14.2145
kc1	12.3223	12.3215	12.0853
quake	47.2477	47.6466	46.5596
space_ga	12.3794	12.7126	<u>11.8971</u>
splice	3.6050	3.6826	<u>3.2915</u>
kr-vs-kp	0.6250	0.6250	0.6250
hypothyroid(2)	0.2649	0.2649	0.2649
analcata_supreme	0.7398	0.7398	0.6165
waveform-5000(2)	9.7000	9.1000	9.4000
delta_ailerons	5.9607	5.9607	<u>5.8906</u>
isolet	2.9487	2.9125	<u>2.6923</u>
puma32H	8.5418	7.8487	<u>7.5046</u>
cpu_small	7.6876	7.4394	<u>7.1995</u>
puma8NH	<u>16.6565</u>	16.9588	<u>16.6565</u>
cpu_act	6.5284	6.4814	5.7962
jm1	17.7768	17.4707	17.5011
sylva_prior	0.4515	0.4925	0.3821
letter(2)	0.0500	<u>0.0250</u>	<u>0.0250</u>
house_16H	9.8969	9.8224	<u>9.6555</u>
kropt	10.9230	7.1768	8.6778
adult-census	13.1276	12.8646	12.7284
amazon_employee	4.7452	4.6271	<u>4.5926</u>
mv	0.0368	0.0368	0.0123
adult	13.9011	13.9622	<u>13.8499</u>
mnist_784	1.4429	1.3976	1.3286
vehicle_sensIT	12.7220	12.4078	12.3211
covertype	9.5792	11.5766	9.0991

Table 12: Test Error(%) - CLS(Part III): The test score for each method. The best methods per dataset are shown in bold, while the second-best methods are underlined.

Datasets	Single-Best	EO	Autostacker	OptDivBO	ES	CMAES	ALL-ES-L1
strikes	3.4118e+05	3.4072e+05	3.3048e+05	3.3038e+05	3.3111e+05	3.0473e+05	3.2037e+05
disclosure_x_noise	8.4511e+08	8.4815e+08	8.5393e+08	8.5419e+08	8.7719e+08	8.8265e+08	8.2596e+08
disclosure_z	6.2967e+08	5.9922e+08	6.7199e+08	6.2887e+08	7.6631e+08	7.6327e+08	6.2287e+08
stock	2.7339e-01	3.0387e-01	3.2874e-01	3.0445e-01	2.9844e-01	3.0871e-01	3.1732e-01
socmob	1.0809e+02	<u>1.0937e+02</u>	2.6734e+02	1.7550e+02	1.1101e+02	1.1292e+02	1.7066e+02
Moneyball	4.5700e+02	8.2509e+02	4.6171e+02	4.5645e+02	4.3366e+02	<u>4.4980e+02</u>	4.5700e+02
insurance	1.8019e+07	1.8779e+07	1.7728e+07	<u>1.7609e+07</u>	1.8966e+07	1.9077e+07	1.8069e+07
weather_izmir	1.4356e+00	1.6041e+00	1.4121e+00	1.3884e+00	1.3880e+00	1.3947e+00	1.3697e+00
us_crime	1.8158e-02	1.7748e-02	1.8093e-02	1.8443e-02	1.7185e-02	<u>1.7254e-02</u>	1.7655e-02
debutanizer	4.3706e-03	3.6395e-03	3.5604e-03	3.7100e-03	3.8771e-03	3.8058e-03	3.9273e-03
space_ga	1.0894e-02	9.5217e-03	8.7566e-03	8.7410e-03	9.0999e-03	9.5045e-03	8.7747e-03
mtp	1.2382e-02	1.2274e-02	1.1829e-02	1.2209e-02	1.1864e-02	1.2054e-02	1.1889e-02
wind	8.7384e+00	8.7125e+00	8.2138e+00	8.2040e+00	8.2374e+00	8.3029e+00	8.1847e+00
bank32nh	6.2034e-03	6.1807e-03	5.8875e-03	6.0119e-03	5.7367e-03	5.6970e-03	5.7160e-03
bank8FM	9.3215e-04	1.0966e-03	8.8017e-04	8.8556e-04	9.0094e-04	9.0198e-04	8.8128e-04
cpu_act	6.9071e+00	6.1408e+00	5.5837e+00	4.8873e+00	5.4768e+00	5.2258e+00	5.4218e+00
cpu_small	8.3812e+00	8.6239e+00	7.9154e+00	7.9213e+00	7.6868e+00	7.8099e+00	7.7066e+00
kin8nm	7.1055e-03	9.8226e-03	5.0617e-03	<u>4.9591e-03</u>	6.2153e-03	6.8652e-03	6.3535e-03
puma32H	5.0607e-05	6.1511e-05	4.8155e-05	4.7037e-05	4.9707e-05	4.9512e-05	4.8388e-05
puma8NH	1.0025e+01	1.0540e+01	9.9420e+00	9.8439e+00	9.8239e+00	9.8729e+00	9.8330e+00
sulfur	7.4291e-04	<u>6.2906e-04</u>	8.6869e-04	9.2979e-04	6.0697e-04	6.5443e-04	6.7434e-04
rainfall_bangladesh	1.5629e+04	<u>1.5449e+04</u>	1.4735e+04	<u>1.4692e+04</u>	1.5351e+04	1.5342e+04	1.5270e+04
kc_house_data	1.9822e+10	1.8827e+10	2.0677e+10	<u>1.8813e+10</u>	1.9452e+10	1.9954e+10	1.9868e+10
house_8L	7.7687e+08	7.6990e+08	7.4949e+08	7.7509e+08	7.4441e+08	7.5221e+08	7.4307e+08
NewFuelCar	6.4424e-02	6.5676e-02	5.7260e-02	5.6136e-02	5.7617e-02	5.7621e-02	5.7079e-02
electricity_prices_ICON	4.3738e+02	4.2373e+02	4.0376e+02	3.8563e+02	4.0931e+02	4.0980e+02	4.1112e+02
OnlineNewsPopularity	6.7930e+07	6.7818e+07	6.7858e+07	6.7858e+07	6.7661e+07	6.7636e+07	6.7509e+07
2dplanes	9.9194e-01	4.3553e+00	9.9361e-01	9.9224e-01	9.9162e-01	<u>9.9165e-01</u>	9.9206e-01
mv	6.5792e-03	6.5792e-03	1.7953e-03	<u>1.7268e-03</u>	2.9186e-03	3.9138e-03	2.2636e-03
black_friday	1.1918e+07	1.1918e+07	1.1895e+07	1.1817e+07	1.1833e+07	1.1831e+07	<u>1.1817e+07</u>

Table 13: Test Error - REG(Part I): The test score for each method. The best methods per dataset are shown in bold, while the second-best methods are underlined.

Datasets	ALL-ES-L2	ALL-Linear-L1	ALL-Linear-L2	BEST-ES-L1	BEST-ES-L2	BEST-Linear-L1
strikes	3.1170e+05	<u>3.0639e+05</u>	1.0279e+06	3.2392e+05	3.2338e+05	3.2621e+05
disclosure_x_noise	8.6024e+08	8.1313e+08	8.6291e+08	<u>8.2466e+08</u>	8.5209e+08	8.2637e+08
disclosure_z	5.9914e+08	6.1621e+08	<u>5.9904e+08</u>	6.1290e+08	6.1917e+08	6.1421e+08
stock	3.2968e-01	3.1504e-01	3.3426e-01	2.6611e-01	2.5553e-01	2.6503e-01
socmob	1.2850e+02	1.6114e+02	1.2702e+02	2.0405e+02	2.0284e+02	1.8475e+02
Moneyball	4.5700e+02	4.6038e+02	4.5565e+02	4.5700e+02	4.5700e+02	4.5401e+02
insurance	1.7691e+07	1.8086e+07	1.7632e+07	1.7875e+07	1.7726e+07	1.7860e+07
weather_izmir	1.3768e+00	<u>1.3715e+00</u>	1.3770e+00	1.4216e+00	1.4115e+00	1.3996e+00
us_crime	1.7625e-02	1.7658e-02	1.7621e-02	1.7744e-02	1.7913e-02	1.7792e-02
debutanizer	3.5519e-03	3.8544e-03	3.5098e-03	4.9969e-03	3.5002e-03	4.7827e-03
space_ga	<u>8.1149e-03</u>	8.4248e-03	8.1879e-03	9.0069e-03	8.3849e-03	8.9144e-03
mtp	1.1819e-02	1.1858e-02	1.1805e-02	1.1969e-02	1.1755e-02	1.1939e-02
wind	<u>8.0532e+00</u>	8.1497e+00	8.0664e+00	8.5639e+00	8.5666e+00	8.5599e+00
bank32nh	5.7391e-03	5.7144e-03	5.7371e-03	5.6783e-03	5.7042e-03	<u>5.6925e-03</u>
bank8FM	8.6807e-04	8.8070e-04	8.6854e-04	9.0888e-04	8.9631e-04	9.1144e-04
cpu_act	4.2041e+00	5.4098e+00	4.2214e+00	5.3814e+00	<u>4.2026e+00</u>	5.1073e+00
cpu_small	6.1522e+00	7.7043e+00	<u>6.1565e+00</u>	7.0833e+00	6.2068e+00	7.0343e+00
kin8nm	5.0694e-03	6.0920e-03	<u>5.0629e-03</u>	6.9057e-03	5.3107e-03	6.4907e-03
puma32H	4.7965e-05	4.8519e-05	4.8045e-05	4.8455e-05	4.7824e-05	4.8868e-05
puma8NH	9.7711e+00	9.7532e+00	<u>9.7689e+00</u>	9.8977e+00	9.8063e+00	9.8508e+00
sulfur	7.5556e-04	6.8126e-04	7.5840e-04	7.0458e-04	7.2464e-04	6.9111e-04
rainfall_bangladesh	1.5373e+04	1.5281e+04	1.5408e+04	1.5417e+04	1.4941e+04	1.5397e+04
kc_house_data	2.1081e+10	1.9768e+10	2.1064e+10	1.9560e+10	1.9502e+10	1.9900e+10
house_8L	7.5804e+08	7.4421e+08	7.5797e+08	7.5197e+08	7.5404e+08	7.4965e+08
NewFuelCar	<u>5.4681e-02</u>	5.6992e-02	5.4533e-02	5.8940e-02	5.8370e-02	5.8970e-02
electricity_prices_ICON	3.8141e+02	4.1110e+02	<u>3.8131e+02</u>	4.1964e+02	3.9244e+02	4.1944e+02
OnlineNewsPopularity	6.7155e+07	6.7675e+07	6.7540e+07	6.7707e+07	6.7869e+07	6.7728e+07
2dplanes	1.0750e+00	9.9207e-01	1.0752e+00	9.9183e-01	9.9585e-01	9.9172e-01
mv	1.8193e-03	2.2777e-03	1.8124e-03	3.0865e-03	2.1893e-03	2.9955e-03
black_friday	1.1981e+07	1.1817e+07	1.1978e+07	1.1895e+07	1.1896e+07	1.1898e+07

Table 14: Test Error - REG(Part II): The test score for each method. The best methods per dataset are shown in bold, while the second-best methods are underlined.

Datasets	BEST-Linear-L2	AutoGluon-	PSEO
strikes	3.2460e+05	3.1159e+05	3.1458e+05
disclosure_x_noise	8.5190e+08	8.5873e+08	8.4298e+08
disclosure_z	6.1692e+08	5.9697e+08	6.1043e+08
stock	<u>2.5841e-01</u>	3.2961e-01	2.9864e-01
socmob	2.0080e+02	1.2468e+02	1.3939e+02
Moneyball	4.5371e+02	4.5700e+02	4.5461e+02
insurance	1.7729e+07	1.7691e+07	1.7543e+07
weather_izmir	1.4111e+00	1.3766e+00	1.3758e+00
us_crime	1.8002e-02	1.7653e-02	1.7698e-02
debutanizer	3.4669e-03	<u>3.1567e-03</u>	3.0108e-03
space_ga	8.3903e-03	8.1136e-03	8.7202e-03
mtp	<u>1.1738e-02</u>	1.1875e-02	1.1614e-02
wind	8.5606e+00	8.0476e+00	8.1334e+00
bank32nh	5.6977e-03	5.7386e-03	5.7100e-03
bank8FM	8.9523e-04	<u>8.6743e-04</u>	8.6717e-04
cpu_act	4.2022e+00	5.4057e+00	4.8873e+00
cpu_small	6.2091e+00	7.5701e+00	7.4696e+00
kin8nm	5.2556e-03	5.0111e-03	4.8166e-03
puma32H	4.7801e-05	4.8314e-05	<u>4.7045e-05</u>
puma8NH	9.8042e+00	9.8319e+00	9.7779e+00
sulfur	7.2344e-04	6.6906e-04	6.6811e-04
rainfall_bangladesh	1.4921e+04	1.5370e+04	1.4598e+04
kc_house_data	1.9581e+10	1.9839e+10	1.8714e+10
house_8L	7.5418e+08	<u>7.4225e+08</u>	7.3476e+08
NewFuelCar	5.7688e-02	5.7062e-02	5.5005e-02
electricity_prices_ICON	3.9112e+02	3.8040e+02	3.8629e+02
OnlineNewsPopularity	6.7851e+07	6.7501e+07	<u>6.7486e+07</u>
2dplanes	9.9713e-01	1.0671e+00	9.9183e-01
mv	2.2100e-03	1.7811e-03	1.7101e-03
black_friday	1.1900e+07	1.1967e+07	1.1795e+07

Table 15: Test Error -REG(Part III): The test score for each method. The best methods per dataset are shown in bold, while the second-best methods are underlined.